International Journal of Nanomedicine Dovepress

Open Access Full Text Article ORIGINAL RESEARCH

Locally Acting Budesonide-Loaded Solid Self-Microemulsifying Drug Delivery Systems (SMEDDS) for Distal Ulcerative Colitis

Hany SM Ali[1,2], Ahmed F Hanafy[3], Rawan Bafail[1], Hamad Alrbyawi[1], Marey Almaghrabi[1], Yaser M Alahmadi[4], Samar El Achy[5]

[1]Department of Pharmaceutics and Pharmaceutical Industries, College of Pharmacy, Taibah University, Madinah, Al-Madinah Al-Munawwarah, Saudi Arabia; [2]Department of Pharmaceutics, Faculty of Pharmacy, Assiut University, Assiut, Egypt; [3]Research and Development Department, Al Andalous Pharmaceutical Industries, Giza, Egypt; [4]Department of Pharmacy Practice, College of Pharmacy, Taibah University, Madinah, Al-Madinah Al-Munawarah, 30001, Saudi Arabia; [5]Department of Anatomical Pathology, Faculty of Medicine, University of Alexandria, Alexandria, Egypt

Correspondence: Hany SM Ali, Email hsali@taibahu.edu.sa, hafandy2000@yahoo.com

Background: Budesonide (BUD) is a BCS class II medication with poor water solubility and limited oral bioavailability. In this study, innovative solid self-microemulsifying drug delivery systems (BUD-SMEDDS) were developed for effective local management of distal ulcerative colitis (UC).

Methods: Based on solubility and emulsification tests, the components of the self-microemulsifying drug delivery system (SMEDDS) were Capryol™ 90, Tween 80, and Transcutol HP. The impacts of BUD-SMEDDS ingredients (as inputs) on the average globule size (AGS), polydispersity index (PDI), and self-emulsification time (SET) as responses were investigated using the Box–Behnken design methodology. Solid rectal systems were then fabricated using the optimized values of SMEDDS components in Lutrol® bases. The developed systems were evaluated for in vitro characteristics and in vivo efficacy using a rat colitis model.

Results: For all responses, the greatest impact was attributed to the oil content of SMEDDS. An optimized BUD-SMEDDS with AGS of 33 ± 2.9 nm, PDI of 0.29 ± 0.03 and SET of 25 ± 2.5 s) was selected for rectal formulations. The developed formulations demonstrated acceptable physical characteristics and mucoadhesive abilities. Differential scanning calorimetric (DSC) analysis revealed the absence of BUD crystallinity in the SMEDDS formulations. The drug release patterns could be regulated by selecting the grade and composition of the incorporated Lutrols. Clinical and histopathological assessments revealed considerable improvements in animals treated with BUD-SMEDDS formulations.

Conclusion: Overall findings confirmed the superior capability of solid SMEDDS as BUD carriers to manage distal colitis in tested animals.

Keywords: Budesonide, SMEDDS, Ulcerative colitis, Box Behnken design, efficacy

Introduction

Ulcerative colitis (UC) is a chronic inflammatory GIT disorder of unknown pathogenesis that affects the colon and rectum.[1] UC is characterized by intermittent flares of active disease with diarrhea, rectal bleeding, and rectal urgency broken by periods of remission.[2] Distal forms of UC include ulcerative proctitis (UP) and ulcerative proctosigmoiditis (UPS) are found in nearly 50% of UC patients.[3] Immunosuppressive drugs, anti-TNF, and, more recently, anti-integrin therapies are commonly used to treat moderate to severe UC.[4] Oral corticosteroids are effective in treating acute flares but have little effects on sustaining remission.[5] Nonetheless, caution is required to avoid unwanted systemic effects.[6]

Budesonide is one of the potent corticosteroids used in colitis management.[7] Consistent with the biopharmaceutics classification system, budesonide is a class II medication (log p = 3.2) with poor water solubility (28 µg/mL).[8–10] When used as a native form, BUD is quickly absorbed in the proximal gastrointestinal tract and subjected to extensive first-pass metabolism leading to a limited systemic bioavailability (6–8%).[9,11] This poses a challenge for its use in UC where

Received: 20 July 2024
Accepted: 4 November 2024
Published: 13 November 2024

delivery in sufficient concentrations to the site of inflammation is crucial. Topical treatment with BUD enema has been studied for the management of active distal UC.[12] However, many patients were found to have problems to retain the liquid enemas. To overcome this problem, rectal foams have also been developed. Small volumes of foam with high viscosity may favor retention and acceptance relative to the administration of high volumes of liquid enema.[13] However, adverse effects like decreased blood cortisol, adrenal insufficiency, and nausea were reported with administration of rectal foams.[14]

Self-microemulsifying drug delivery systems (SMEDDS) are valuable for addressing the problems of formulating drugs with limited water solubility. In SMEDDS, isotropic mixtures of oils, surfactants, and co-surfactants can generate oil-in-water nanoemulsions when mildly agitated in aqueous media such as GI fluids.[15] The minute droplets of the generated nanoemulsions present lipophilic drugs in dissolved forms with a wide interfacial area for beneficial absorption and subsequent augmented bioavailability.[16] Nonetheless, there are certain disadvantages to use standard liquid self-emulsified systems. During storage, the medicine or its components may precipitate, interact with packaging materials, and cause instability. Conversion into solidified forms combines the benefits of liquid self-emulsified preparations; such as improved bioavailability with those of solidified formulations; as improving formulation stability, allowing for accurate dosing, and increasing patient compliance.[17,18]

Response surface methodology (RSM) is a collection of statistical methods for developing and analysing the relationship between responses and variables. The Box-Behnken design (BBD) has been employed successfully in pharmaceutical research because of its great ability to shorten experimentation times and reduce expenses compared to traditional procedures.[19] Generally, the BBD requires three independent variables, each with three levels. All experiments should have factor levels at low and high extremes, in addition to a one-factor level in the center.[20]

The current study aims to exploit the advantages of stable solid SMEDDS formulations to provide sufficient local concentrations of the poorly water-soluble drug (BUD) at inflamed colitis sites. To achieve that, the Box–Behnken design was utilized to optimize SMEDDS preparation with the desired values of globule size, polydispersity and self-emulsification ability. The optimized preparation was subsequently incorporated within Lutrol® bases to fabricate solid rectal formulations of BUD SMEDDS. The mucoadhesive properties imparted by the Lutrol® bases help prolong and limit the topical BUD effect. The fabricated rectal systems were characterized by in vitro and in vivo performance.

Methodology

Materials

Budesonide (BUD) was obtained from Acros Organics (Geel, Belgium). Propylene glycol dicaprylate/dicaprate (Labrafac™ PG), Caprylocaproyl macrogol-8-glyceride (Labrasol®), Labrafac Lipophile, and propylene glycol monocaprylate (Capryol™ 90) were purchased from UFC Biotechnology (Amherst, NY, USA). Oleic acid was obtained from Merck KGaA (Darmstadt, Germany). Polyoxyl 40 hydrogenated castor oil (Cremophor® RH 40), polyethylene glycol 400 (PEG 400), Polyoxyethylene-20-sorbitan monooleate (Tween 80), Lutrol® F68, and Lutrol® F127 were purchased from Sigma-Aldrich Chemie GmbH (Steinheim, Germany). Diethylene glycol monoethyl ether (Transcutol HP) was purchased from Gattefossé (Cedex, France). Suppocire CS2X was supplied by Gatefossé (Lyon, France). Ultrapure water was obtained using a Millipore water filtration system (Bedford, MA, USA). The rest of ingredients were of pharmaceutical quality and were utilized as supplied.

Assay of BUD

BUD was quantified by a validated HPLC assay using a Hypersil® C18 column.[21] The mobile phase (ethanol–acetonitrile–phosphate buffer, prepared at 2:30:68, v/v/v, pH 3.4) was delivered at a flow rate of 1.5 mL / minute with UV detection at 240 nm.

Solubility Studies

The solubility of BUD in the different components was evaluated using shake-flask procedures.[22,23] Briefly, known excess quantities of BUD (100 mg) were introduced into vials containing certain amounts (2 g) of the excipient and

vortexed for 5 min. vials were kept in thermostatically controlled water bath at 37 ± 1 °C with continuous shaking (100 rpm) for two days, followed by an equilibrium period of one day. Supersaturated samples were centrifuged at 10,000 × g for 15 min (Centrifuge Z 206 A; Hermle Labortechnik GmbH, Wehingen, Germany). The supernatant was filtered through a 0.45 µm membrane filter, followed by appropriate dilution with methanol. The dissolved BUD was quantified as described in assay of BUD.

Emulsification Proficiency

Some typical non-ionic surfactants (Cremophor® EL, Cremophor® RH 40, Span 80, Tween 20, 40, 60 and 80) were tested, as shown below, to explore their emulsifying capabilities towards Capryol™ 90.

Emulsification of the Greatest Portion of Oil

The chosen oil (Capryol™ 90) was slowly incorporated into surfactant solutions (10 mL of 10% w/v aqueous solution) by vortex mixing until hazy appearance.[24]

Transparency and Emulsification Ease

In separate glass vials, the oil: surfactant (1:1 w/w ratio) mixture was mixed with heating in a water bath at 50 °C and homogenized by Ultra Turrax IKA 10T (IKA®-Werke GmbH, Staufen, Germany) at 2000 rpm for 2 minutes. The mixtures were then diluted with distilled water in a volumetric flask. The inversions necessary to obtain a homogeneous emulsion within the flasks were used to assess the ease of emulsion formation. After standing for 2 h, the % transmittance (% T) was measured at a maximum wavelength of 650 nm. Spectra were recorded using a UV-1650 PC UV-visible spectrophotometer (UV6100 PC, EMC Lab, Germany) against a blank of deionized water.[25]

Pseudo-Ternary Phase Diagram

Several mixtures including different quantities of selected SMEDDS components (oil, surfactant, and co-surfactant) were initially prepared. The mixture (1 g) was slowly titrated against double-distilled water and gently mixed at room temperature under magnetic stirring. Self-microemulsion development was considered when the system became transparent or a slightly yellow to light-blue milk solution.[26] The phase boundary was identified by observing the change in appearance of the sample from clear to turbid. The ProSim software (ProSim, Toulouse, France) was used to depict the relevant weight ratios of the components and construct a pseudo-ternary phase diagram.[18]

Box-Behnken Design (BBD)

BBD was used to optimize the SMEDDS by Design–Expert 13 software (Stat–Ease, Inc., Minneapolis, MN, USA). The design matrix includes 15 runs of budesonide microemulsions (BUD-ME1 to BUD-ME15), as shown in Table 1 and Table 2. The amounts of Capryol™ 90 (X_1, 100–150 mg), Tween 80 (X_2, 150–250 mg), and Transcutol HP (X_3,

Table 1 Variables and Levels of the Box-Behnken Design

Variables	Coded levels		
Independent Variables	**Low (−1)**	**Intermediate (0)**	**High (+1)**
A: (Amount of oil (mg)	100	125	150
B: Amount of surfactant (mg)	150	200	250
C: Amount of Cosurfactant (mg)	50	65	80
Dependent variables		Target	
R_1 = Average globule size (nm)		Minimize	
R_2 = Polydispersity index		Minimize	
R_3 = Self emulsification time (s)		Minimize	

Table 2 Randomized Experiments of the Box–Behnken Design

Run code	A	B	C	R_1 (nm)	R_2	R_3 (s)
BUD-ME 1	150	200	80	97 ± 8	2.0 ± 0.33	125 ± 14
BUD-ME 2	125	250	50	38 ± 4	0.85 ± 0.15	40 ± 3.7
BUD-ME 3	100	200	80	45 ± 6	0.23 ±0.04	39 ± 4.2
BUD-ME 4	125	200	65	58 ± 7	0.86 ±0.07	47 ±3.9
BUD-ME 5	150	150	65	120 ± 14	2.8 ± 0.40	135 ± 12
BUD-ME 6	150	250	65	113 ± 9	1.4 ±0.22	122 ±9.8
BUD-ME 7	125	200	65	63 ± 8	0.89 ±0.08	49 ±5.3
BUD-ME 8	125	250	80	48 ± 6	1.1 ±0.21	57 ±6.2
BUD-ME 9	150	200	50	87 ± 9	1.7 ±0.14	98 ±8.2
BUD-ME 10	100	250	65	21 ± 3	0.23 ±0.03	22 ± 1.9
BUD-ME 11	100	150	65	90 ± 10	1.36 ±0.19	87 ±7.3
BUD-ME 12	125	150	80	105 ± 8	2.1 ±0.14	116 ±10.6
BUD-ME 13	125	200	65	55 ± 7	0.9 ±0.11	50± 3.8
BUD-ME 14	100	200	50	22 ± 4	0.25 ±0.04	26 ±3.1
BUD-ME 15	125	150	50	78 ± 9	2.2 ±0.04	69 ±4.9

Note: Capryol™ 90 (A), Tween 80 (B), Transcutol HP (C).
Abbreviations: Average globule size (AGS, R_1), Polydispersity index (PDI, R_2), Self-emulsification time (SET, R_3).

50–80 mg) were used as factors. These factors varied at the low (coded as −1), middle (coded as 0), and high (coded as +1) levels. Three replicated center points (X_1 = 125 mg, X_2 = 200 mg, and X_3 = 65 mg) were used to uniformly estimate the prediction variance over the design space.[20] Response surface explorations were performed to reveal the impacts of changing the studied factors on the observed responses: average globule size, AGS (R_1), polydispersity index (PDI) (R_2), and self-emulsification time, SET(R_3). The target of BBD was to minimize R_1, R_2 and R_3. Weighed quantities of BUD were initially dissolved in oil, blended with the surfactant and co-surfactant, and stirred to obtain a homogeneous mixture. The developed SMEDDS was stored in glass bottles at room temperature until further use. The preparations were observed for alterations such as turbidity or phase separation. The polynomial equation (1) is used for the fitness of the responses and model generation:

$$R_i = \beta_0 + \beta_1 A + \beta_2 B + \beta_3 C + \beta_4 AB + \beta_5 AC + \beta_6 BC + \beta_7 A^2 + \beta_8 B^2 + \beta_9 C^2$$

Where R_i is the dependent variable, β_0 is the intercept, and β_1–β_9 denote the regression coefficients calculated from the observations of individual responses. A, B, and C represent fixed independent variables. The other terms AB, AC, BC, A^2, B^2, and C^2 depict the interaction of the factors and their quadratic terms, respectively. Significance of the generated models was estimated using Analysis of Variance (ANOVA), lack-of-fit test, and multiple correlation coefficient (R^2) test. The optimal components of the SMEDDS were selected using the desirability function of the generated models.[27–29] For model validation, a statistically adjusted formulation was experimentally developed and characterized for the AGS, PDI, SET, and zeta potential (ZP). Data are reported as means ± SD.

AGS and PDI

AGS and PDI of the prepared microemulsions (MEs) were determined by Microtrac S3500 (Microtrac Inc., Montgomeryville, PA, USA) after appropriate dilution with double distilled water to avoid the effect of multiple scattering. AGS and PDI were measured thrice for 120 s at 25 °C, and average values were displayed.[30,31]

Self-Emulsification Time (SET)

SET was used to judge the spontaneity of emulsification of the developed batches. SET is the time elapsed by the SMEDDS to create homogeneous dispersions when diluted in an aqueous solution.[29] A specified volume (1 mL) of BUD-SMEDDS batches was gradually added to a phosphate buffer solution (250 mL, pH 6.8, 37 ± 0.5 °C) in a standard

USP type II dissolution apparatus. Gentle agitation was maintained by rotating the paddles at 50 rpm, and SET was recorded.

Zeta Potential

Microtrac S3500 (Microtrac Inc., Montgomeryville, PA, USA) was employed to measure Zeta potential of optimized budesonide microemulsion (OBM). The preparations were diluted 10 times prior to testing.[27]

Thermodynamic Stability Testing of the Optimized SMEDDS

Firstly, the optimized BUD microemulsion (OBM) formulation was subjected to six cycles of refrigeration at 4 °C, heating to 45 °C, and storage for 48 h. The OBM was then tested by centrifugation at 3500 rpm for 30 min (Centrifuge Z 206 A; Hermle Labortechnik GmbH, Wehingen, Germany). The OBM was finally exposed to freeze–thaw cycles (n = 3) at −21 °C and 25 °C, with storage at each temperature for 48 h.[32,33] The instability signs (phase separation or precipitation), ADS, and PDI were evaluated after each stability assessment.[29]

Preparation of Solid BUD-SMEDDS Rectal Formulations

The fusion melting method was employed to prepare the solid rectal BUD formulations. Bases consisting of Lutrol® F68 (F1), Lutrol® F127 (F2) and their 50% combination (F3) were used to assess their suitability for accommodating the optimized BUD-SMEDDS. In a dish over water bath, calculated amounts of Lutrol F68, F127, or their 50% mix were firstly melted. The optimized BUD-SMEDDS was added under continuous stirring (Table 3). Homogeneous dispersions were introduced into stainless steel suppository molds (4 mL capacity). A conventional BUD formulation was prepared similarly using Suppocire® CS2X as a fatty base. The prepared suppositories for all formulations weighed 3.5 ± 5% g with a 3 mg BUD content.

In vitro Pharmacotechnical Assessment

The color, clarity, and consistency of the produced suppositories were visually evaluated as intact units by longitudinal breakage after removal from the mold. The lack of fissuring, pitting, fat blossoming, exudation, sedimentation, and migration of the distributed BUD was also evaluated. The developed suppositories were evaluated for uniformity of weight and BUD content according to the BP (British Pharmacopoeia). Mechanical strength was evaluated using an Erweka breaking strength tester (Erweka GmbH, Heusenstamm, Germany). To determine the pH, the formulations were dissolved in warm water, followed by filtration, and the pH of the filtrate was measured using a calibrated digital pH meter.[34,35]

Assessment of Mucoadhesive Properties

The mucoadhesive forces of preparations (F1-F4) were assessed using a previously reported procedure[36,37] with slight modifications (Figure 1). The model tissues were fresh sections of cow distal colon mucosa collected from a local

Table 3 Composition of Budesonide Rectal Formulations

Ingredients (mg)	Codes			
	F1	F2	F3	F4
Budesonide	3	3	3	3
Capryol™ 90	105	105	105	–
Tween 80	236	236	236	–
Transcutol HP	70	70	70	–
Lutrol F68	3086	–	1543	–
Lutrol F127	–	3086	1543	–
Suppocire® CS2X	–	–	–	3497

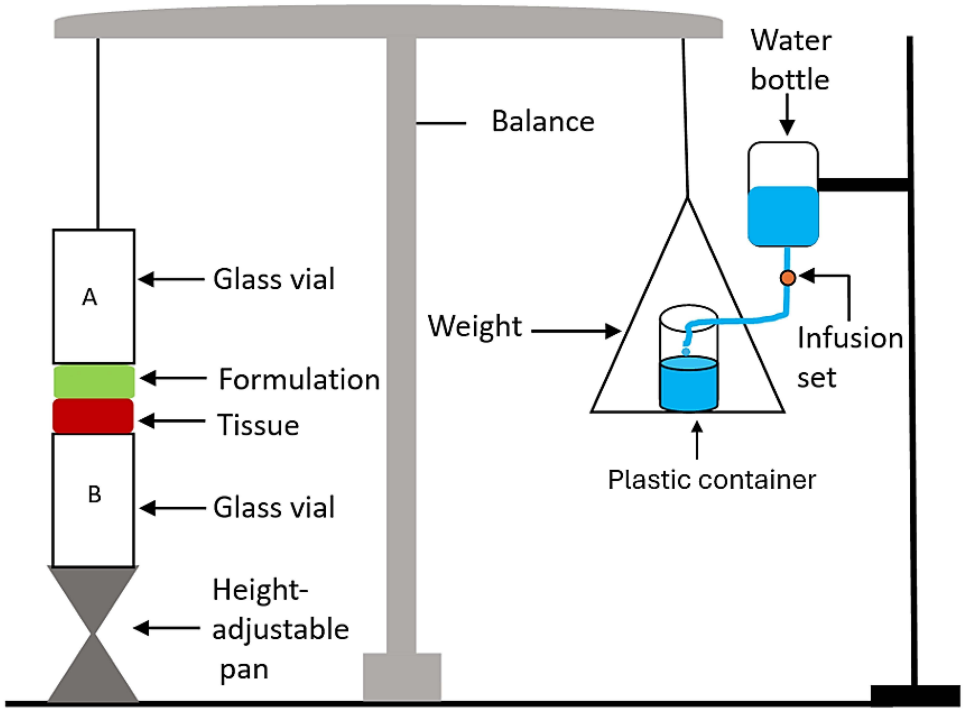

Figure 1 Illustration of the device used to evaluate mucoadhesive forces.

slaughterhouse and kept in normal saline at 4 °C. Formulations sections (1 cm^2) were attached to the cap of a glass vial (A) using scotch tape and connected to a balance. Colon mucosa was securely fitted into another glass vial (B) using a rubber band and kept located on a height-adjustable pan. The two vials were then carefully positioned to allow adherence between tested formulations and colon mucosa. A fixed weight was put on the upper vial for 2 minutes to allow uniform attachment between the mucosa and tested formulations. Water droplets were allowed to fall, via a rate controlling infusion set, in a plastic container on the other side of the balance. The weight of water droplets increased until detachment occurred between the formulation and tissue. The mucoadhesive strength (dyne.cm^{-2}) according to Equation 2.[36]

$$Mucoadhesivestrength = m.g/A$$

where m is the water weight (g), g is the acceleration due to gravity (980 cm.sec^{-2}); and A is the area of the utilized mucosa (cm^2).

Differential Scanning Calorimetry (DSC)

Thermal profiles of raw BUD, Lutrol® F86, F127 and the prepared BUD-loaded SMEDDS formulations (F1-F3) were obtained using a Netzsch thermal analyzer (Netzsch F3 Maia®, Germany). Specific quantities of the tested samples were placed in tightly sealed aluminum pans. Samples were placed in DSC chamber and exposed to heating runs over a temperature range of 25–350 °C at a heating rate of 5 °C/min.[38]

Drug Release

The patterns of BUD release from formulations (F1-F4) were depicted using a USP XXIII dissolution device type II paddle (Pharma Test, Hainburg, Germany). The release media were phosphate buffer (900 mL at pH 7.5) maintained at 37 ± 0.5 °C and stirred using paddles (100 rounds per minute). Samples of 5 mL were drawn at specified times and replaced with the corresponding volumes of the release solution to ensure constant liquid volumes. The samples were centrifuged and quantified for BUD using HPLC procedures (Assay of BUD). The percentage of BUD released was calculated and plotted as a function of time. All measurements were performed in triplicates.

Release Kinetic Modelling

Several kinetic models have been used to process the generated results and explore the mechanisms of BUD release. The developed plots included zero-order, first-order, Higuchi, Korsmeyer-Peppas, and Hixson-Crowell cube root models.[39] All models were constructed and validated up to release of 60% of the loaded dose.[40] To identify the mechanism of drug release, the exponent "n" was derived using the slope of the straight line of Korsmeyer-Peppas plot.

In vivo Assessment

Experimental Animals

Ethical approval for all the animal experiments were obtained from the Institutional Review Board (College of Pharmacy, Taibah University) before starting the experiments (Project reference number COPTU-REC-78-20230909). In vivo studies were carried out in accordance with the recommendations for laboratory animal care and use provided in the National Academies Press's Guide for the Care and Use of Laboratory Animals, 8th edition, Washington, DC, USA. The study required the use of twenty male Sprague Dawley rats (200–220 g) for in vivo testing. The animals were acclimatized in a room with a regulated-temperature (24 ± 1 °C) and maintained at 12-hour light/dark cycle ad standard rodent pelleted diet was supplemented by ad libitum access.

Induction of Colitis

The acetic acid colitis model was used in this study because of its similarities to human colitis in terms of pathogenesis, histological appearance, and associated proinflammatory mediators.[41,42] Animals were fasted for 16 h before testing, with free access to water, and were then anesthetized with ketamine (50 mg/kg) and xylazine (10 mg/kg). A polyethylene tube (2 mm diameter) was introduced via the rectum into the colon at 6 cm. Each animal received a single rectal dose of acetic acid of 1 mL (4%, v/v in 0.9% saline) via a polyethylene tube (2 mm in diameter) for 30s for colitis induction.

Experimental Design

Twenty rats were grouped into four collections. In group I, saline was administered to the rat colons in the same manner as acetic acid (normal control). Group II was the colitis control group (BUD-free SMEDDS formulations). Groups III and IV were treated with the conventional BUD formulation without the self-emulsified system (BUD-CF-treated group) or optimized BUD-SMEDDS formulation, respectively. The rats were kept under observation for three days following the induction of colitis without treatment to develop a state of typical colitis. On the 4th day, groups III and IV were treated with their corresponding BUD formulations at a dose of 3 mg/kg/day twice daily for nine days. A blank SMEDDS formulation with the same regimen was administered to group II.

Clinical Colitis Scoring

The magnitude of induced colitis was determined by calculating the disease activity index (DAI) using changes in body weight of rats bodies, consistency of fecal traits, and the degree of hematochezia.[43] Table 4 displays the criteria for calculating the DAI.[44] The sum of individual scores yielded an overall DAI ranging from 0 (healthy) to 12 (maximal colitis activity). DAI was checked on days 0, 3, 6, 9 and 12 by an investigator who was blinded to the research groups. On day 13, rats were slaughtered to assess the progress of various treatments. Following separation, colons were put on non-absorbing surfaces. The colon lengths and ratios between wet colon weights to the corresponding total body weights were used as an metrics to quantify the severity of colitis.[44]

Microscopic Assessment

Samples from distal colons of the rats were fixed in neutral buffered formaldehyde (10%) overnight. The samples were dehydrated in an ascending series of ethanol solutions, followed by clearance in xylene and paraffin embedding. Thick sections (5 μm) were prepared and stained with hematoxylin and eosin (H&E). Masson's trichrome staining was performed to assess the presence or absence of fibrosis. A histopathologist, blinded to the treatment regimens, assessed the stained sections. A scoring system for colitis based on the Geboes Score (with modifications) was developed, which assesses the five main tiers of colitis, including architectural changes, chronic inflammatory infiltrates, eosinophils, and neutrophils within the lamina propria, cryptitis, erosions, and ulcerations.[45]

Table 4 The Disease Activity Index (DAI) Scoring System

Loss of Weight Range	Score	Consistency of Fecal Traits Criteria	Score	Degree of Hematochezia Criteria	Score
None	0	Consistent pellets	0	No blood in hemoccult	0
1–5%	1				
5–10%	2	Pasty stools not maintained in the anus	2	Positive hemoccult	2
10–20%	3				
> 20%	4	Diarrhea	4	Significant bleeding	4

Stability Checking

Samples of the chosen formulation were kept in dark containers covered with aluminum foil and stored at 25 ± 2 °C and ambient relative humidity. The impact of storage on appearance, BUD content, AGS after reconstitution, PDI, ZP, and the drug release percent after 120 minutes (% $Q_{120\ min}$) for 6 months. The stability was evaluated by comparing the original results with the post-storage results.

Statistical Analysis

The findings were analysed using Student's *t*-test and one-way analysis of variance (ANOVA), followed by the least significant difference test (LSD). Differences were considered significant when *p*-values were less than 0.05. The GraphPad Prism 8.0 (San Diego, CA, USA) was used to conduct statistical analysis.

Results and Discussion

Solubility Screening

The optimal choice of SMEDDS constituents is critical for achieving the maximum drug payload, solubility, and system stability.[46] In the current study, the choice of oil constituent was carried out based on the capacity to solubilize the greatest quantity of BUD. The saturated solubility of BUD in the assessed SMEDDS constituents is shown in figure 2. Of the oils tested, Capryol™ 90 displayed the greatest BUD solubilization; hence, it was recommended as the oil component of the system. Capryol™ 90 is an amphiphilic medium-chain triglyceride with eight carbons that can function as a surfactant and self-emulsifier.[47] Furthermore, similar aliphatic chains in BUD and Capryol™ 90 induced stacking, in addition to the dipole-dipole interactions between their carbonyl groups.[48]

Selection of Surfactant/Co-Surfactant Mix

To facilitate oil dispersibility during microemulsion (MEs) production, emulsifiers (s) must be capable of minimizing the interfacial tension to a very low value. Non-ionic surfactants are usually preferred to formulate SMEDDS because they are less affected by pH changes and are usually considered safe and biocompatible. Although the drug solubilization potential is vital in selecting SMEDDS components, it is not the sole factor that dictates the choice of emulsifier(s) in the generated systems. More critical consideration has been given to the emulsifying proficiency of the surfactant towards the chosen oily phase.[24] The respective values of flask inversions involved in ME formation and % T were used to assess the capacity of the surfactant to produce MEs and to evaluate the stability of the formed MEs.[33] Figure 3A shows the % T and flask inversion values for the various MEs. Of the examined surfactants, Span 80 showed the greatest number of flask inversions (14 inversions), suggesting a difficulty in the emulsification process. ME created using Labrasol® showed the lowest stability, with a % T of 66%. In contrast, emulsion production using Tween 80, Tween 20, Cremophor® RH 40, and Cremophor® EL as emulsifying agents required only five, six, six, and seven flask inversions, respectively, suggesting the ease of emulsification. Besides, the % T of the created emulsions reached 97–99%, indicating a good stability of the formed ME. Changes in the structure and chain length are crucial for detecting variations in the emulsification efficacy of surfactants.[49] Furthermore Tween 80 showed the highest capacity (2.7 ± 0.24 g) to emulsify

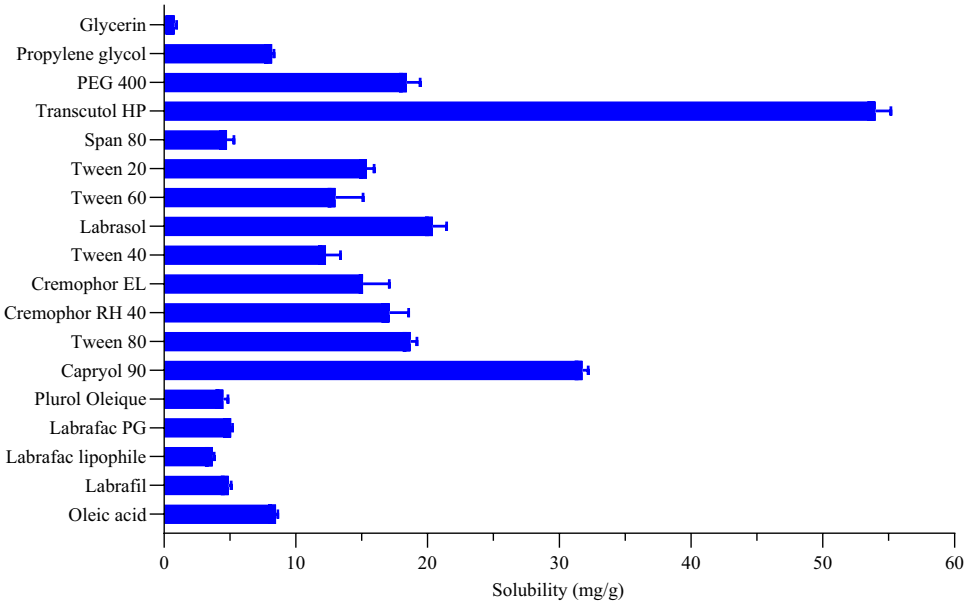

Figure 2 Results of solubility of budesonide in tested vehicles.

Capryol™ 90 (Figure 3A). Based on emulsifying proficiency findings, Tween 80 was used for oil emulsification in this study. Furthermore, the inclusion of a co-surfactant is usually required in SMEDDS formulations to enhance the emulsification capacity of the chosen surfactant. An appropriate co-surfactant can reduce the interfacial tension, fluidize the hydrocarbon portion of the interfacial layer, and enhance the emulsification spontaneity. In this study, the tested co-surfactants were individually mixed with Tween 80 at a fixed (1:1, W/W) surfactant: co-surfactant ratio. The findings evidently demonstrated that Capryol™ 90 underwent the greatest emulsification, as reflected by the high % T, low flask inversions and high oil capacity values, with Transcutol HP as a co-surfactant (Figure 3B). Moreover, as portrayed in solubility results, BUD revealed excellent solubility in Transcutol HP. When the surfactant and co-surfactant show good solubilization capacities for the drug, this could represent an additional advantage in preventing drug precipitation during storage.[24]

Pseudo Ternary Phase Diagram

Based on previous screening criteria, BUD-SMEDDS was designed to include Capryol™ 90, Tween 80, and Transcutol HP. To designate the boundaries of the self-emulsifying zones and adjust the concentrations of the previously chosen vehicles, a pseudo-ternary phase diagram was created (Figure 4). The shaded area represents the self-emulsification area, where the production of clear ME is spontaneous with no phase separation. The region around the shaded area shows a combination of weak emulsion formation abilities and higher droplet size. Satisfactory spontaneous emulsification did not occur efficiently when the surfactant content was lower than Capryol™ 90. The maximum self-emulsifying zone was observed at a S_{mix} (surfactant: co-surfactant, W/W) ratio of 3: 1. This is plausibly explained by the greater content of Tween 80 in the S_{mix} ratio 3:1 in comparison to the other ratios, 2:1 and 1:1 (data not shown). Co-surfactants are useful for forming ME in appropriate amounts. Nonetheless, excess quantities of the co-surfactant decrease the stability of the emulsion because of its inherently high aqueous solubility and induced size enlargement owing to the growing interfacial film.[50] After delineating the ME area in the phase diagram, the limits of the independent variables were chosen for further optimization using BBD.

Box Behnken Design (BBD)

The BBD was created to investigate the cumulative influence of the three processing factors on the three responses of the BUD-SMEDDS; AGS (R_1), PDI (R_2), and SET (R_3). Table 1 and 2 list the BBD matrices based on the run order and

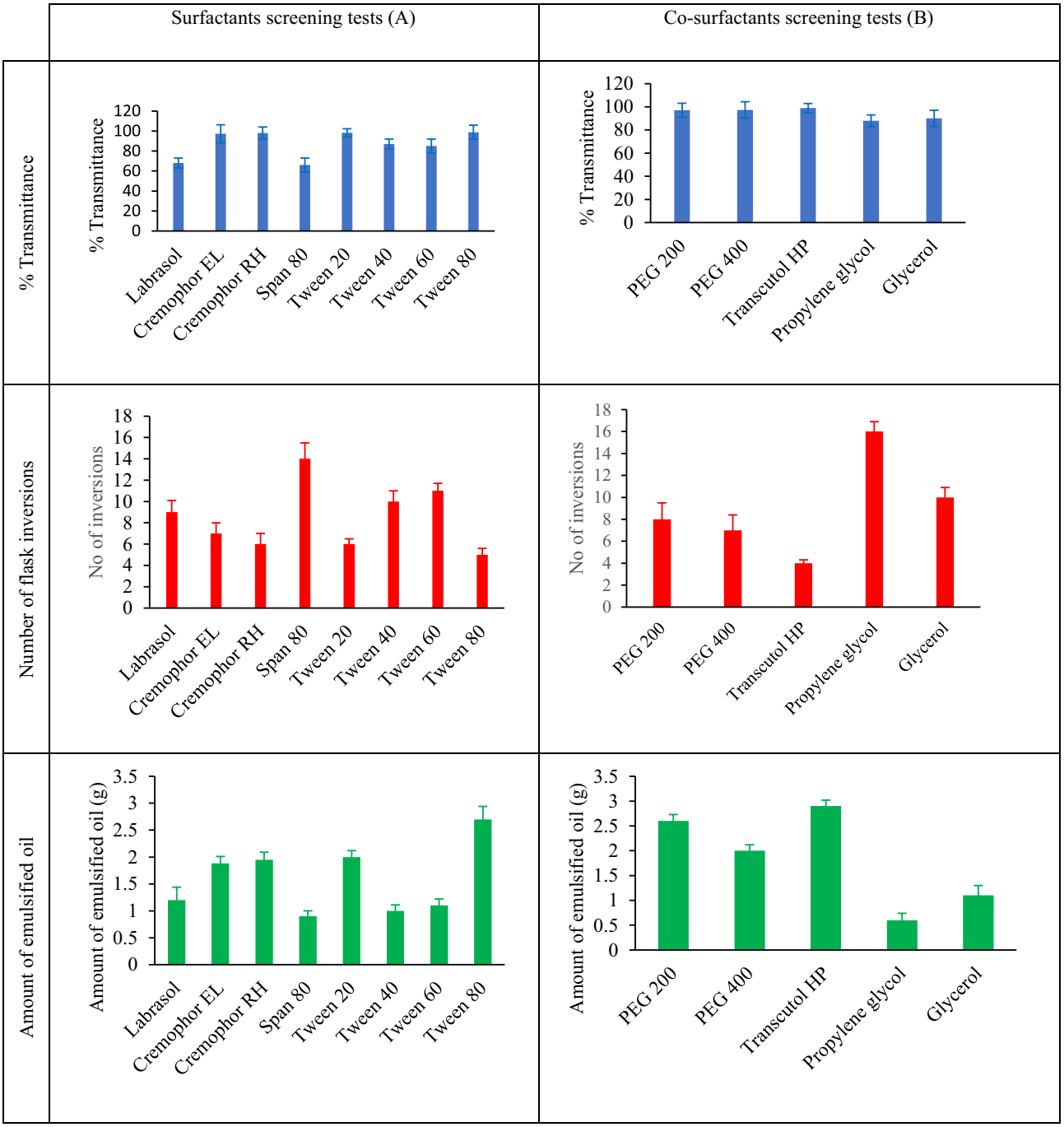

Figure 3 Results of surfactants (**A**) and co-surfactants (**B**) screening for oil emulsification.

observed responses. AGS, PDI and SET revealed notable changes in the generated batches with respective ranges; 21 ± 3–120 ± 14 nm (for AGS), 0.23 ± 0.03–2.8 ± 0.40 (for PDI) and 22 ± 1.9 to 135 ± 12s (for SET) indicating remarkable influences of the evaluated factors on the designated responses. Design Expert software offered ANOVA, a lack-of-fit test, and multiple correlation coefficient (R^2) tests to assess the significance of the generated models (Table 5). The *p* values of the models must be < 0.05, which is the best fit to the quadratic model[51] and was confirmed by the *p*-values for responses R_1, R_2 and R_3 (Table 5). A lack-of-fit test implies data variation around fitted values. However, the Probe>F value in the lack-of-fit tests part of should be determined as insignificant ($p > 0.05$) when compared to the pure error.[29] The measured responses revealed an insignificant lack of fit for the values (Table 5). The multiple correlation coefficient

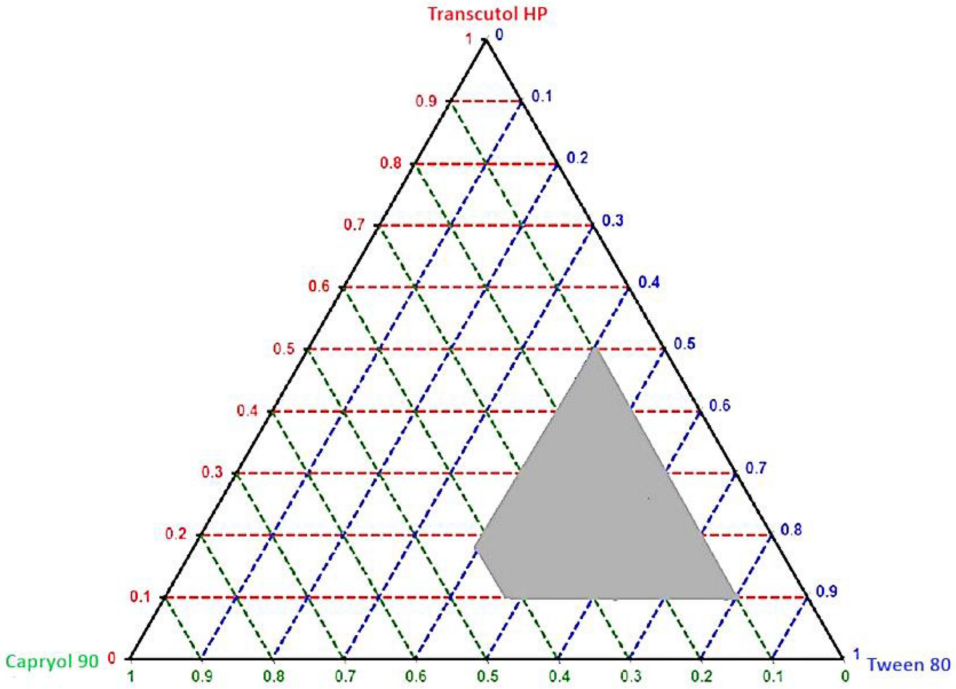

Figure 4 A pseudo ternary diagram depicting the self-emulsification region (the shaded area).

(R^2) denotes the magnitude of variation around the mean, with acceptable and desired values of > 0.6 and > 0.9, respectively.[52] The corresponding R^2 values for R_1, R_2 and R_3 are 0.9275, 0.9582, and 0.9246, respectively, indicating good confidence in the predictability of the regression Equations. The coefficients AB, AC, BC, A^2, B^2, and C^2 specify the interaction and quadratic effects, respectively. Generally, low *p*-values and high F-values had a profound influence on the response variables of the model terms. Contour plots of Transcutol HP, with all responses, showed parallel lines, indicating that the co-surfactant has the least ability to cause changes in the studied responses.

Response Surface Analysis

Model polynomial equations were used to generate graphs of the three-dimensional response surface. Such graphs are also useful for assessing the influence of two separate variables on the responses at the same time. In all figures, the third variable remained constant at the middle level (Figures 5–7).

AGS

AGS is an important parameter in designing drug-loaded SMEDDS. A faster release rate and higher interfacial area for drugs to be absorbed are associated with smaller sizes. The effects of variables A, B, and C on the response (AGS, R_1) are shown in Figure 4. The following quadratic polynomial equation for AGS is shown in equation 3:

$$AGS\ (R_1, nm) = 58.67+29.87A-21.63\ B + 8.75\ C - 4.25\ BC +11.42\ A^2 +15.92\ B^2 -7.33C^2$$

The preceding equation expresses the quantitative influence of the variables (A, B, C) and their interaction coefficients (AB, AC, BC) on the AGS response. When the coefficient values of the relevant model components of the equation were compared, variables A and B had the highest influence on the AGS, whereas BC had the least significant impact. As described, Capryol™ 90 was selected as the oil carrier for the BUD. Capryol™ 90, with an HLB of 4–5, has been efficiently utilized in various SMEDDS formulations.[53] Regression analysis for AGS showed a positive sign for A (oil content), suggesting that AGS was synergistically affected by the oil content (A). Systems containing a high percentage of oil-generated ME with larger droplets (Figure 5A and B). This may be attributed to the distortion of the interfacial layer by the entry of oil droplets into the surfactant chain, which in turn affects the surface curvature of the

Table 5 Statistical Analysis of the Models Generated by Box-Behnken Design

Fitting Model	Factors	Coefficient	P-value	ANOVA
Average globule size (AGS)	Intercept	58.67	< 0.0001	F = 84.98 R^2 = 0.9935 Adjusted R^2 = 0.9818 Predicted R^2 = 0.9275 Model *p* value < 0.0001 *p* value of lack of fit = 0.4779
	A (Capryol 90)	29.87	< 0.0001	
	B (Tween 80)	−21.63	0.0022	
	C (Transcutol HP)	8.75	0.0008	
	AB	15.50	0.1920	
	AC	−3.25	0.1057	
	BC	−4.25	0.0038	
	A^2	11.42	0.0009	
	B^2	15.92	0.0222	
	C^2	−7.33	< 0.0001	
Polydispersity index(PDI)	Intercept	0.8833	< 0.0001	F = 204.97 R^2 = 0.9973 Adjusted R^2 = 0.9924 Predicted R^2 = 0.9582 Model *p* value < 0.0001 *p* value of lack of fit = 0.0569
	A(Capryol 90)	0.6987	< 0.0001	
	B(Tween 80)	−0.6163	0.0412	
	C(Transcutol HP)	0.0650	0.0633	
	AB	−0.0800	0.0285	
	AC	0.1025	0.0482	
	BC	0.0875	0.8565	
	A^2	−0.0067	< 0.0001	
	B^2	0.5833	0.0410	
	C^2	0.0958	< 0.0001	
Self-emulsification time (SET)	Intercept	48.67	< 0.0001	F = 112.65 R^2 = 0.9951 Adjusted R^2 = 0.9863 Predicted R^2 = 0.9246 Model *p* value < 0.0001 *p* value of lack of fit = 0.0681
	A(Capryol 90)	38.25	< 0.0001	
	B(Tween 80)	−20.75	0.0005	
	C(Transcutol HP)	13.00	0.0022	
	AB	13.00	0.1813	
	AC	3.50	0.0209	
	BC	−7.50	0.0002	
	A^2	22.17	0.0003	
	B^2	20.67	0.6402	
	C^2	1.17	< 0.0001	

droplets, causing their enlargement.[54] Surfactant concentration (B) was the second most important variable influencing the size of the generated globules. The negative sign of B in equation 3 suggests an antagonistic influence of the surfactant concentration on AGS. A noticeable reduction in the AGS was observed with increasing surfactant levels (Figure 5A–C). The surfactant plays a crucial role in determining globule size in emulsion formation. Low levels of

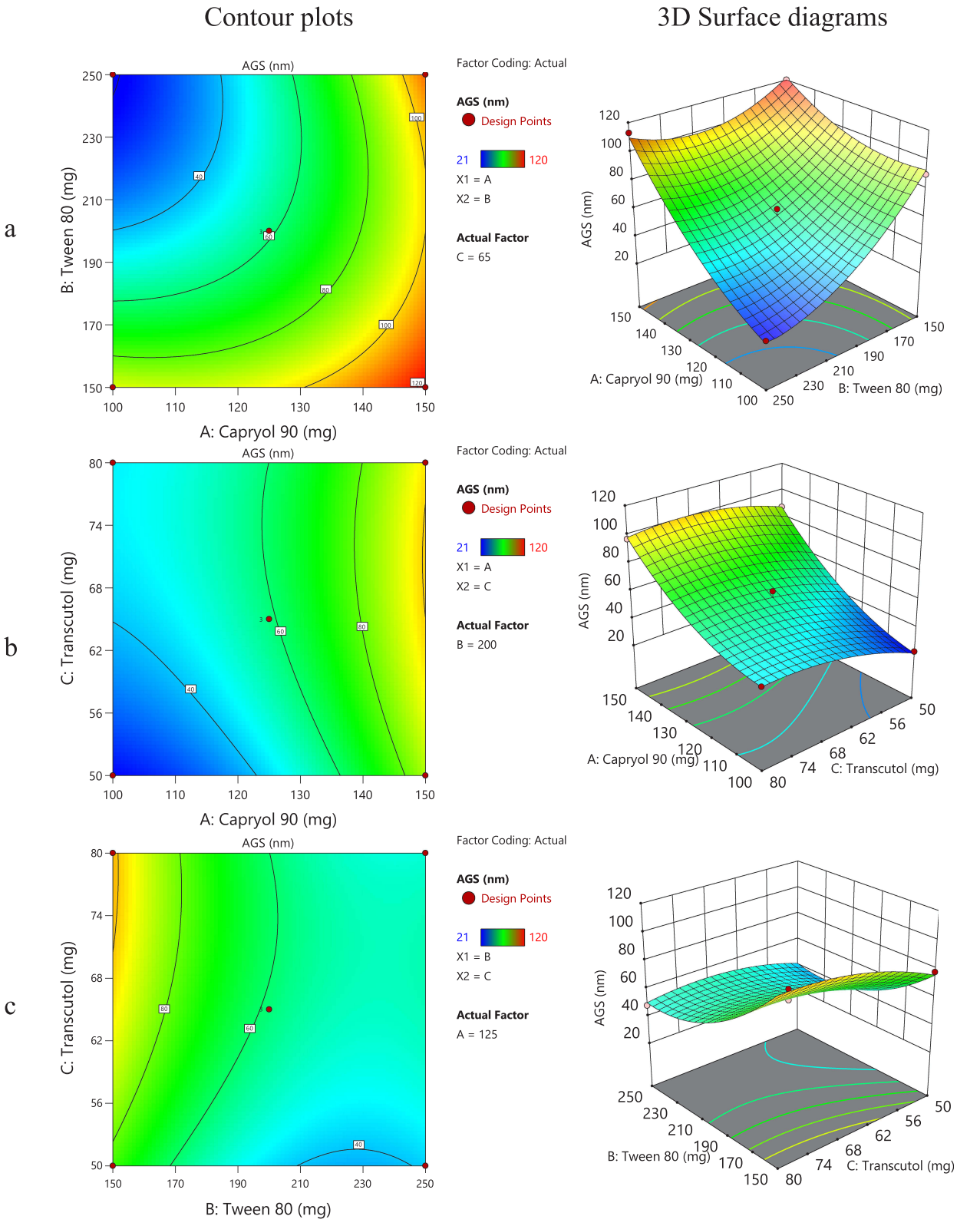

Figure 5 Contour and response surface plots of interactions between oil–surfactant (**a**), oil–cosurfactant (**b**) and surfactant–cosurfactant (**c**) and the average globule size (AGS).

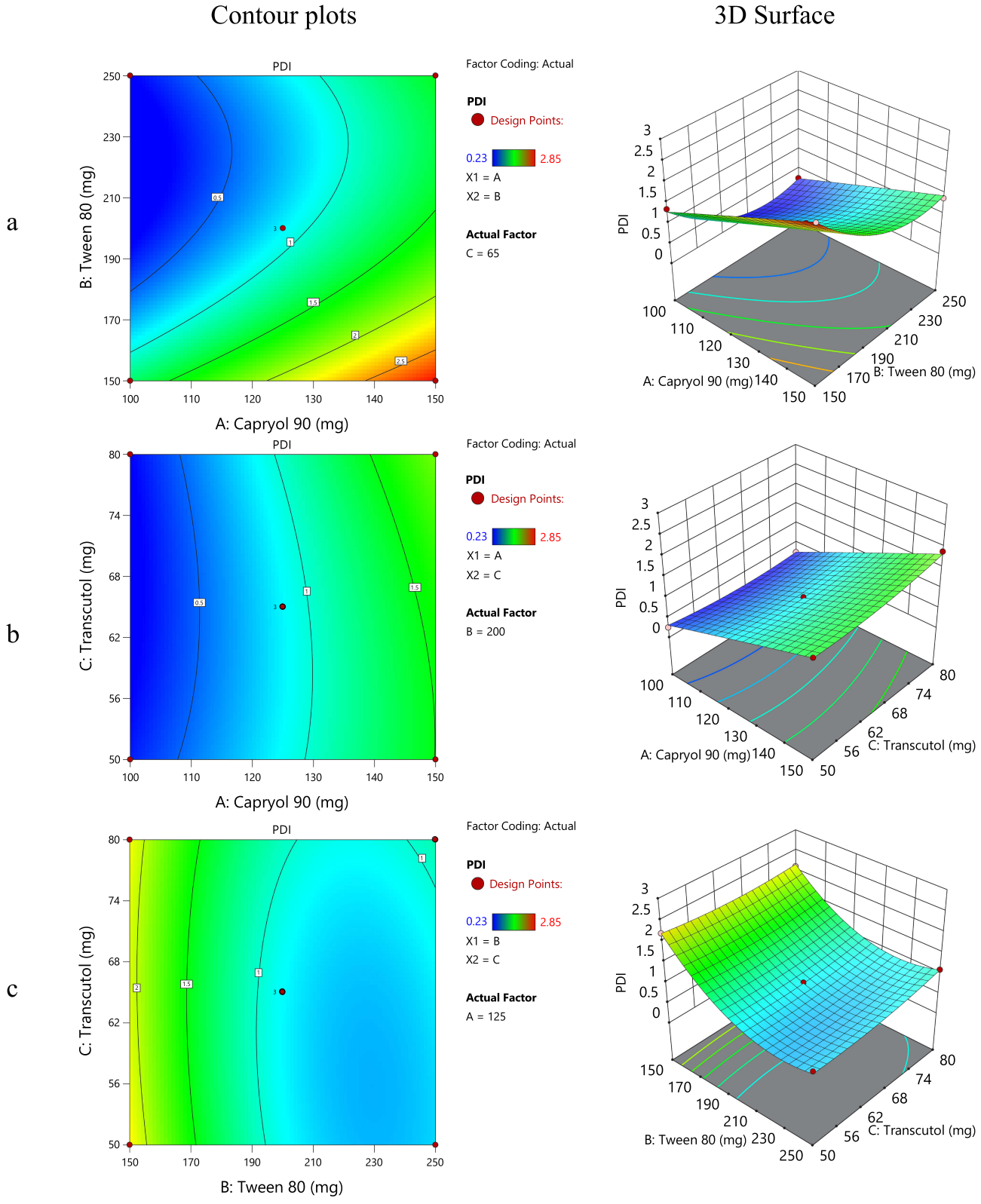

Figure 6 Contour and response surface plots of interactions between oil–surfactant (**a**), oil–cosurfactant (**b**) and surfactant–cosurfactant (**c**) and polydispersity index (PDI).

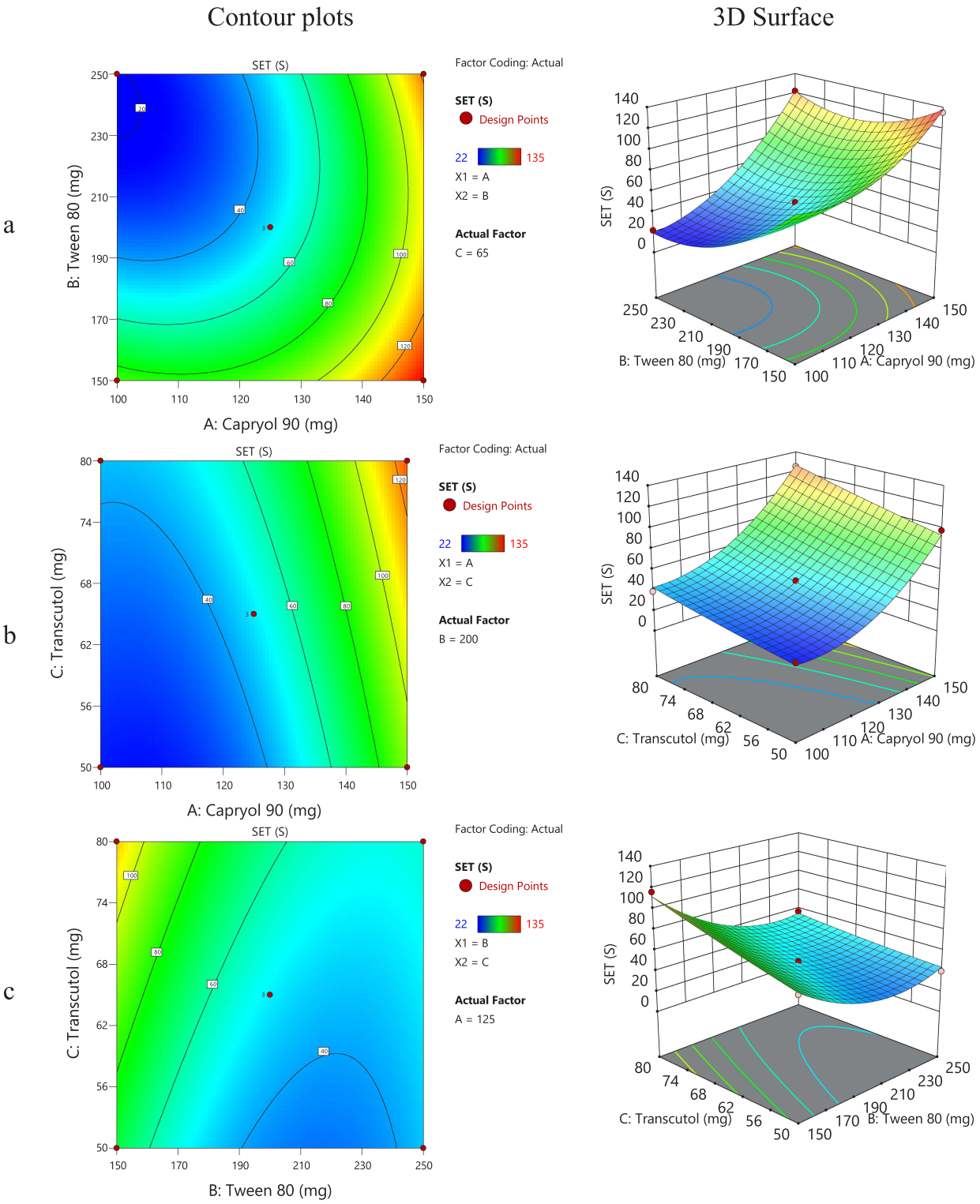

Figure 7 Contour and response surface plots of interactions between oil–surfactant (**a**), oil–cosurfactant (**b**) and surfactant–cosurfactant (**c**) and self-emulsification time (SET).

surfactants in the system were inadequate for oil droplet coverage, prompting their coalescence and enlargement. By increasing its concentration, the surfactant is densely packed at the interfacial surfactant layer and stabilizes the oil globules.[20] Equations 4 and Figure 5B and C suggest a minor synergistic effect of the co-surfactant on AGS compared to the oil and surfactant contents. It can be deduced that the combination becomes more lipophilic with increasing amounts

of Transcutol HP (HLB = 4),[55] particularly at low amounts of Tween 80, creating difficulty in emulsification and hence increasing particle size.[20]

PDI

The PDI value represents size distribution of ME generated by the SMEDDS. The quadratic polynomial equation for PDI (Equation 4):

$$PDI\ (R_2) = 0.8833 + 0.6987A - 0.6163B - 0.0800\ AB + 0.1025\ AC - 0.0067A^2 + 0.5833\ B^2 + 0.0958\ C^2$$

The quantity of oil (A), amount of surfactant (B), interaction between oil and surfactant (AB), interaction between oil and co-surfactant (AC), and quadratic interaction of oil (A^2), surfactant (B^2), and co-surfactant (C^2) all had a significant effect on the PDI (*P*-value less < 0.05). Nonetheless, the amount of co-surfactant (C) showed a non-significant effect on the PDI. The response surface and control plots for the impact of the variables on the PDI are presented in Figure 6. Upon increasing the oil concentration, the globule sizes became more diverse, as evidenced by the higher PDI values (Figure 6A and B). High oil concentrations produce viscous systems, making the spontaneous breakup of the oil-water interface more difficult.[56] An initial increase in the surfactant content reduced the PDI values (Figure 6A–C). However, the heterogeneity in globule size increased, as observed by the greater PDI values, with a further increase in the surfactant concentration. Higher surfactant contents produced very viscous systems with difficulty in spontaneously rupturing the oil-water interface.[57]

SET

The emulsification rate is a crucial metric for assessing the effectiveness of the emulsification procedures. Production of ME is thermodynamically spontaneous because the free energy required is relatively minimal. When water dilution with mild agitation is applied to SMEDDS, they should disperse fully and promptly. The quadratic polynomial equation of the model is as follows:

$$SET\ (R_3, s) = +48.67 + 38.25A - 20.75B + 13.00\ C + 3.50AC - 7.50BC + 22.17A^2 + 1.17\ C^2$$

According to equation 5, all variables except AB and B^2 showed significant effects on SET (*p*-value less than 0.05). The greatest impacts were linked to oil content (synergistic) and surfactant content (antagonistic). The response surface plot for SET (Figure 7A and B) indicates an increase in emulsification time with increasing oil content. At high oil contents, the increased viscosity of the system impeded the development of the emulsification process. SET was considerably enhanced with increasing surfactant levels. The existence of sufficient amounts of surface-active agents at the oil/water interface decreases the interfacial tension and, as a result, the emulsification time. A similar finding was reported when cephalexin was emulsified using a system composed of lauroglycol 90, poloxamer 188, and Transcutol HP.[58]

Optimization of BUD-SMEDDS

The desirability approach of the Design Expert 13 software was then probed for the simultaneous optimization of AGS, PDI and SET.[30] A desirability value between zero and one indicates the proximity of the response to the established goal values (from least desirable to most desirable). Selection was based on attaining the minimum AGS, PDI, and SET values (Figure 8). The proposed amounts of SMEDDS components were 105 mg, 236 mg and 70 mg of Capryol™ 90, Tween 80, and Transcutol HP, respectively. The overall desirability value is 0.982 (Table 6). The observed values for AGS, PDI, SET, and ZP were 33 ± 2.9 nm, 0.29 ± 0.03, 25 ± 2.5, and − 27 ± 2.4 mV, respectively. As shown in Table 6, the observed values of the investigated responses are reasonably close to the numerically anticipated values provided by the models. The low error values signify that these findings positively support the optimization developed to predict responses within the specified levels of the studied variable.

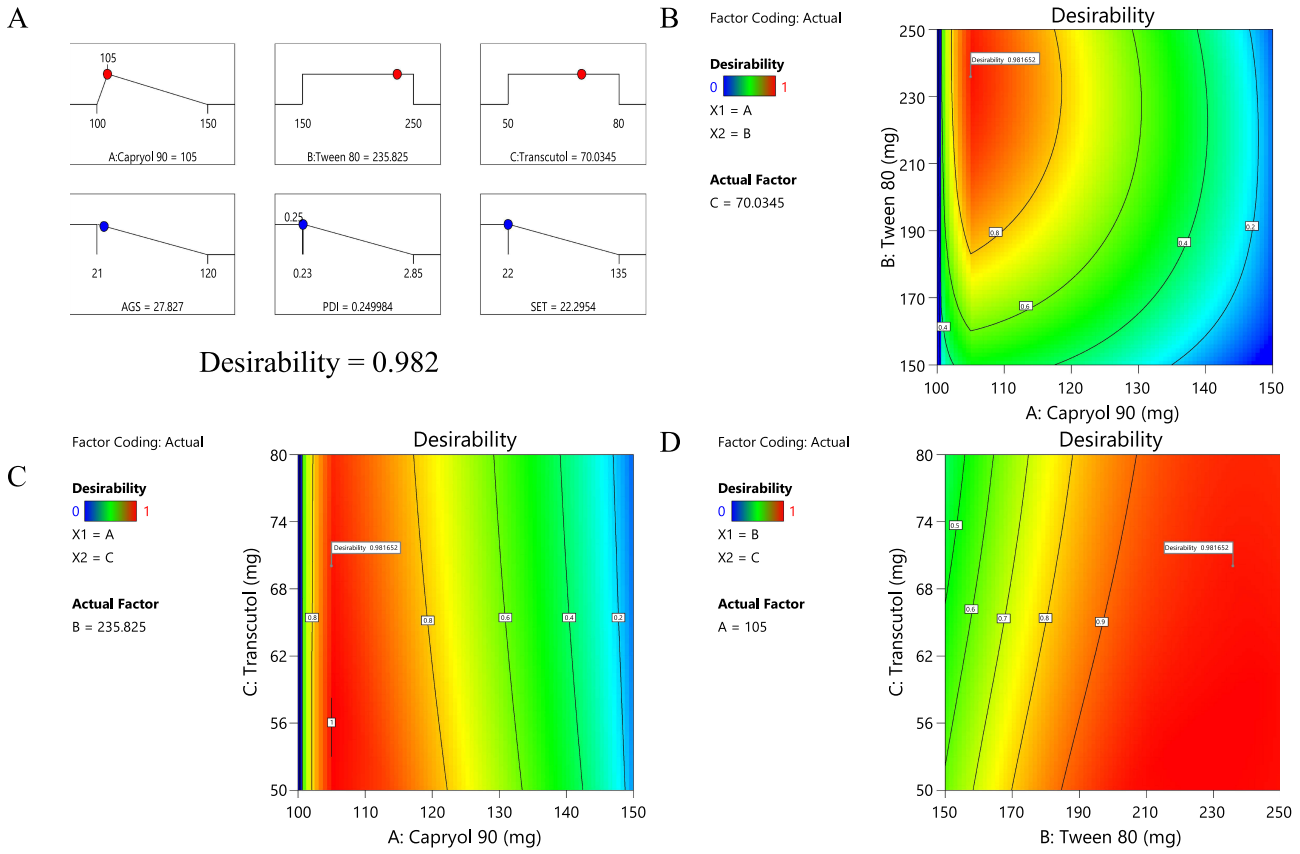

Figure 8 Ramp graph (**A**) and contour plots (**B-D**) of desirability for the numerically optimized BUD-SMEDDS formulation.

Thermodynamic Stability

A stable ME can endure different stress conditions without separating the component phases or precipitating the loaded drug.[29] Table 7 displays the changes in AGS, PDI, and SET after the thermodynamic evaluation. As revealed by findings, the optimized budesonide microemulsion (OBM) showed good stability without demonstrating any precipitation, phase separation or remarkable changes in AGS, PDI or SET following stress tests. In nanomedicine studies, zeta potential (ZP) is considered an important metric for determining the stability of ME. The high ZP value (− 27 ± 2.4 mV) helps stabilize BUD-ME because of the adequate electrostatic repulsion between the droplets.[59]

Table 6 Results of Budesonide Microemulsion Optimization Process

Code	Ingredients (mg)			Response	Predicted	Observed	Error	Desirability
	A	B	C					
OBM	105	235.82	70.03	AGS (nm)	28	33 ± 2.9	17.8	0.982
				PDI	0.25	0.29 ± 0.03	16.0	
				SET (s)	22	25 ± 2.5	13.6	

Note: Capryol™ 90 (A), Tween 80 (B), Transcutol HP (C).
Abbreviation: Optimized budesonide formulation (OBM),Average globule size (AGS), Polydispersity index (PDI), Self-emulsification time (SET).

Table 7 Impacts of Different Stress Conditions on Stability of Optimized Budesonide Microemulsion (BUD-ME)

Parameter	Initial	Centrifugation	Heating/Cooling	Freeze/Thaw
PT (%)	97 ± 7.8	96 ± 8.2	94 ± 9.1	94 ± 8.9
AGS (nm)	33 ± 2.9	35 ± 2.9	36 ± 2.9	38 ± 2.9
PDI	0.29 ± 0.03	0.30 ± 0.04	0.30 ± 0.03	0.31 ± 0.04
SET (s)	25 ± 2.5	27 ± 2.9	27 ± 2.8	29 ± 3.1

Abbreviations: PT (percent transmission %), AGS (Average globule size, nm), SET (self-emulsification time, s), PDI (polydispersity index, value).

Characterization of Rectal Formulations

Lutrols (poloxamers) have been effectively utilized as carriers for SMEDDS formulations because of their safety profiles, biocompatibility, surface activity, and popular use in rectal formulations.[60,61] Lutrols also have cytoprotective and anti-inflammatory properties.[62] In general, the lutrols-based suppositories are uniform in color with a smooth touch without fissuring, pitting, exudation, or drug deposits (Table 8). The loaded BUD (%) ranged from 95 ± 6.7 to 99 ± 2.8, indicating uniform dispersion of the medication. The prepared rectal systems showed good mechanical strengths ranging from 2.8 ± 0.16 to 3.2 ± 0.20 kg/cm^2, signifying acceptable mechanical strength to endure pressures throughout storage and transits. The measured pH values ranged between 6.6 ± 0.70 to 7.2 ± 0.75 making them acceptable for rectal use.

Mucoadhesive Characteristics

Delivery systems with mucoadhesive characteristics maximize local therapeutic concentrations at the target sites.[63] Mucoadhesion is assumed to occur via wetting and adsorption of the formulation on the mucus membrane, with subsequent diffusion and interpenetration of the incorporated polymer into the mucous gel layers.[64] The force by which pharmaceutical systems adhere to mucosal sites is known as the mucoadhesion force. A greater mucoadhesive force resulted in a longer retention of the formulation at the mucoadhesion site. Nevertheless, possible damage to the mucous membrane can occur because of excessive mucoadhesive forces.[61] Thus, the optimized preparation should have the appropriate mucoadhesive characteristics. Table 8 represents the mucoadhesive forces of the evaluated delivery systems. As observed, formulations of Lutrols possessed reasonable mucoadhesive characteristics compared to F4 (12 ± 1.7×10^2 dyne/cm^2). Lutrols can entangle and noncovalently bonded to mucin, thereby promoting a high level of connection with numerous biological membranes.[65] According to the results obtained, the Lutrol F 127-based formulation (F2) showed the highest mucoadhesive force (68 ± 4.1×10^2 dyne/cm^2). This is consistent with the results of previous studies.[66,67] Adhesion via entanglements and van der Waals bonding is enhanced by increasing the molecular weight of the mucoadhesive polymers.[68] The Lutrols F68/F127 hybrid combination (F3) exhibited an intermediate mucoadhesion value (51 ± 3.8×10^2 dyne/cm^2).

Table 8 Characteristics of Budesonide Formulations

Code	Appearance	Weight (g)	Drug content (%)	Crushing strength (kg/cm^2)	pH	Mucoadhesive force (dyne/cm^2)*10^2
F1	Pale yellow	3.5 ± 0.20	95 ± 6.7	2.8 ± 0.16	6.6 ±0.70	34 ± 2.7
F2	White	3.7 ± 0.18	96 ± 3.2	3.2 ± 0.20	6.9 ±0.65	51 ± 3.8
F3	White	3.6 ± 0.22	99 ± 2.8	3.0 ± 0.23	7.1 ±0.54	68 ± 4.1
F4	White	3.7 ± 0.34	98 ± 3.1	2.9 ± 0.31	7.2 ±0.75	12 ± 1.7

DSC Findings

Figure 9 displays the thermal responses of the unprocessed BUD, Lutrol F 68, and F 127, and the tested formulations. The DSC thermogram of unprocessed BUD revealed a sharp endothermic at 260 °C, corresponds to melting of the crystalline drug.[69,70] The DSC curves of Lutrol F 68 and Lutrol F 127 showed strong endothermic peaks at 53.9°C and 62.6°C, respectively. Such peaks appear because of melting of the crystalline components in Lutrols.[71] Incorporating formulation ingredients into F1-F3 resulted in a noticeable reduction in the melting onsets of Lutrol F 68 and F 127. Such ingredients represent as solutes that lower the melting points of the Lutrols.[72] Reducing the onset of melting may be advantageous because it allows instantaneous melting at body temperature. No endotherms corresponding to BUD melting points were detected in the formulation thermograms. These observations indicate that BUD remained dissolved in the components of SMEDDS.

Drug Release

The BUD release from the tested formulations is shown in Figure 10. The comparatively slow BUD release from F4 is mainly explained by the poor aqueous solubility of BUD and the higher affinity of the hydrophobic BUD to the lipophilic base.[8] Nonetheless, an approximately complete release of the loaded BUD was observed within 60 minutes from F1 with no indication of drug precipitation up to 24 h. This can be explained by the rapid collapse and dissolution of the carrier, Lutrol F 68 in this case, and instantaneous dispersion within the release medium. The inclusion of surfactant and a co-surfactant system supported the rapid formation and spreading of O/W ME in the release medium. This increased water penetration into ME droplets with disruption of the interface decreased the droplet size, eventually improving the rate and extent of drug dissolution. On the other hand, when Lutrol® F 127 was utilized as the carrier to fabricate the solid rectal system (F2), a remarkable delay in BUD release was noted (the time required for 50% drug release; $T_{50\%}$ =160 minutes). This can be attributed to the formation of rapid and effective gel layers by the polymer. However, the incorporation of BUD-SMEDS in a hybrid combination of Lutrol® F68 and F127 attenuated BUD release to an intermediate level, with a $T_{50\%}$ = 95 minute. Lutrols (poloxamers) are special types of synthetic tri-block copolymers composed of hydrophobic chains of poly(propylene oxide) units (PPO) located in the middle of two hydrophilic chains of poly(ethylene oxide) units (PEO).[73] Lutrols are readily soluble at low temperatures because of the hydrogen bonding between the PEO and PPO units and water molecules. The breakdown of hydrogen bonds at certain micelle temperatures and poloxamers consolidates and self-assembles to create spherical micelles with a hydrophobic propylene oxide (PO) core. The micelles expanded in size until the PO core

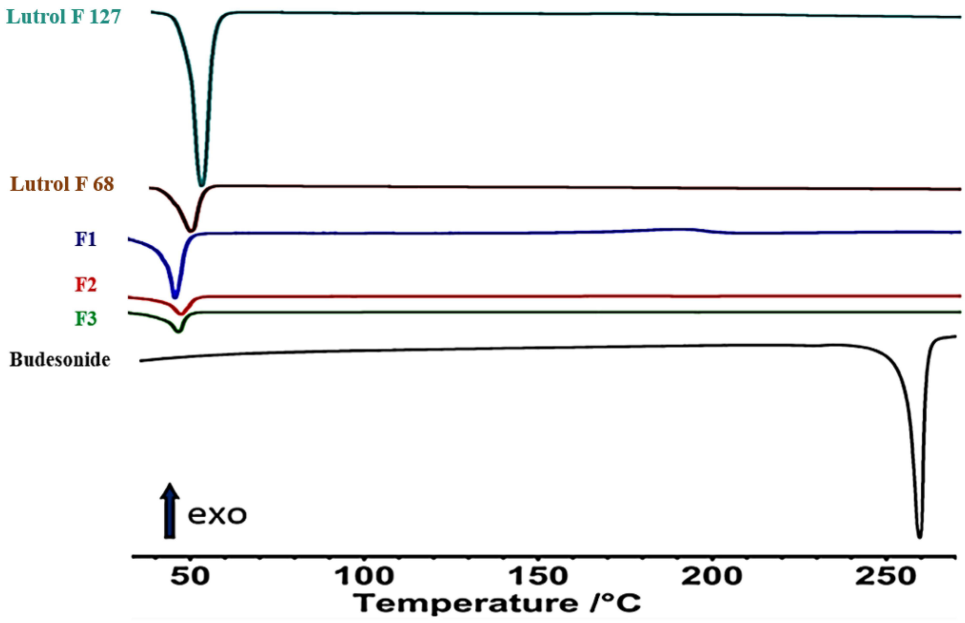

Figure 9 DSC thermograms of unprocessed budesonide, Lutrol® F68, Lutrol® F127 and formulations F1, F2 and F3.

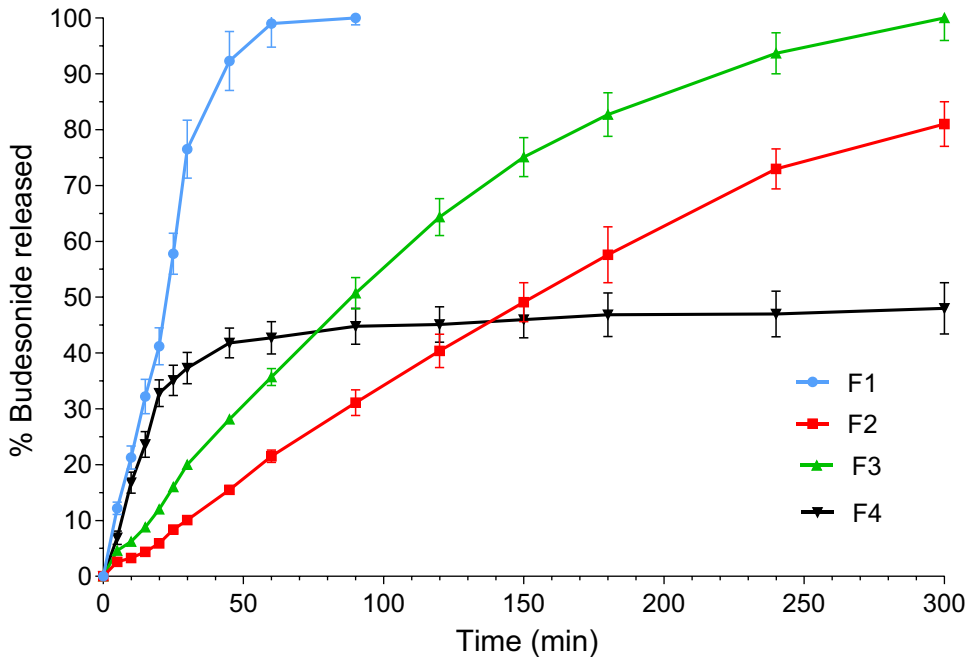

Figure 10 Release of budesonide from tested formulations F1, F2, F3 and F4.

completely dehydrated. The outer hydrophilic chains of the micelles expanded and interacted to generate three-dimensional gels. Lutrol® composition is crucial for altering drug release patterns in gelling devices. The ratio of hydrophobic (PPO) to hydrophilic (PEO) blocks has a considerable influence on the properties of the entire gel and, consequently, on the release of the loaded medications. Increasing the level of hydrophobic components such as Lutrol® F127 can considerably improve gel strength, lower attrition, and impede drug diffusion. Concurrently, the addition of F68 increases the PEO ratio, leading to less entanglement of the micelles.[74] Accordingly, the BUD release profiles of Lutrol®-based SMEDDS formulations can be tuned by selecting both the grade and composition of the polymers.

Mathematical Modelling of BUD Release

The release of various drugs from matrices incorporating swellable polymers, such as Lutrols, is complicated. In such systems, drug transport can be dominated solely by diffusion, erosion, or a mixed pathway of the two processes. According to Korsmeyer–Peppas model, the release exponent "n" reflects pattern of release (as Fickian diffusion (case I), case II transport and anomalous transport).[39] When "n" equal or less than 0.45 denotes traditional Fickian diffusion-controlled (case I) drug release. When "n" = 0.89, this denotes case II relaxational release transport; non-Fickian, zero-order release, whereas "n" > 0.89 designates super case II (enhanced plasticization at the relaxing boundary) patterns. Values of "n" between 0.45 and 0.89 are usually indicative of both processes (drug diffusion within the hydrated matrix and polymer relaxation), which are collectively referred to as anomalous transport.[75] Release Kinetic equations were used to study the BUD release pattern from tested formulations (up to 60% release). Next, an analysis was carried out by applying the models proposed by Korsmeyer–Peppas, which established an exponential relationship between the release and time (Table 9). Applying kinetic models revealed that the Korsmeyer–Peppas equation describes the release of BUD from the conventional oil-based formulation F4 (r^2 =0.866). Here, the "n" value of 0.136 for F4 indicates the Fickian diffusional release kinetics. The Korsmeyer–Peppas equation adequately described BUD release from F1, F2, and F3 with r^2 values of 0.980, 0.996, and 0.998, respectively. The respective "n" values for F1, F2 and F3 were 0.728, 0.918 and 0.887 and 0.918 suggesting an anomalous transport type. Lutrols or poloxamers function via a process of continuous swelling of the polymer and concurrent or eventual dissolution of the polymer.[76]

Table 9 Release Kinetics of Budesonide from Tested Formulations

Code	Zero Order	First Order	Higuchi Model	Hixson- Crowell Model	Korsmeyer–Peppas Model		Release order	Main release mechanism
	(r^2)	(r^2)	(r^2)	(r^2)	(r^2)	(n)		
F1	0.977	0.957	0.976	0.934	0.980	0.728	Korsmeyer–Peppas	Anomalous transport
F2	0.988	0.908	0.968	0.895	0.996	0.918	Korsmeyer–Peppas	Anomalous transport
F3	0.997	0.908	0.967	0.933	0.998	0.887	Korsmeyer–Peppas	Anomalous transport
F4	0.789	0.752	0.845	0.585	0.866	0.136	Korsmeyer–Peppas	Fickian diffusion

Clinical Monitoring

To evaluate colitis throughout the study, the disease activity index (DAI) was computed as a combination of the loss of body weight, consistency of fecal characteristics, and level of hematochezia. Apart from the animals in the healthy control group, a fast increase in the DAI compared to the baseline was observed in the other groups (Figure 11A). However, following the initiation of BUD therapy, the DAI showed a noticeable decrease across animals treated with the reference BUD formulation and BUD-SMEDDS. On day 12, the BUD-SMEDDS-treated group showed a significantly lower DAI value than the untreated colitis group ($p < 0.001$) and the conventionally treated group ($p < 0.01$). BUD therapy considerably reduced colon weight relative to body weight compared to the non-treated colitis ($p < 0.001$) and the reference BUD treated groups ($p < 0.05$) (Figure 11B). Additionally, no significant difference was observed in the weight of the healthy colons ($p > 0.05$), demonstrating an effective reversal of this index. Shortening of colon length is regarded as a sign of experimental colitis.[77] As displayed in Figure 11C, BUD-SMEDDS also considerably enhanced colon lengths compared to the control colitis ($p < 0.001$) and reference BUD treated animals ($p < 0.01$) (Figure 11C).

Histopathology

Figure 12AL shows photomicrographs of H&E-stained sections harvested at the end of the experiment. Colon photomicrographs of the healthy group showed intact surface mucosa and regular mucosal glands with a preserved inflammatory gradient and absence of activity (Figure 12A and B). The colitis control group showed an ulcerated epithelial lining with architectural distortion, mucosal gland and goblet cell depletion, low-grade dysplasia, transmucosal inflammation, and cryptitis (Figure 12D and E). In the group treated with the reference BUD (F4), the colons demonstrated focal surface ulceration with mucosal gland distortion and moderate inflammatory infiltrates including neutrophils and eosinophils (Figure 12G and H). Photomicrographs of BUD-SMEDDS (F3)-treated colons showed intact surface mucosa and regular mucosal glands with preserved goblet cells and mild inflammatory cellular infiltrates in the lamina propria with a preserved inflammatory gradient (Figure 12K and L).

Trichrome staining is a relatively straightforward and frequently used histological method to reveal fibrous tissues with collagens.[78] Trichrome-stained colonic sections revealed the presence of a minimal fibrous tissue component in the healthy group (Figure 12C) and moderate fibrosis in the lamina propria and submucosa in the colitis-induced group (Figure 12F). However, increased fibrosis with a denser collagenic component of the lamina propria and submucosa was noted in transections through the colonic wall of rats in the reference conventional BUD-treated group (Figure 12J). In contrast, the BUD-SMEDDS-treated group exhibited fibre density comparable to that of the healthy control group (Figure 12M).

Geboes Scoring

The total "Geboes" score of the healthy colons studied was 1/16, verifying the absence of evidence of inflammation (Figure 13). Conversely, all acetic acid-exposed blank-treated rats exhibited an elevated colitis rating of 16/16, indicating serious colitis. BUD therapy ameliorates inflammation and damage intensity to scores of 8.4 ± 0.54 and 3.2 ± 0.44 for the

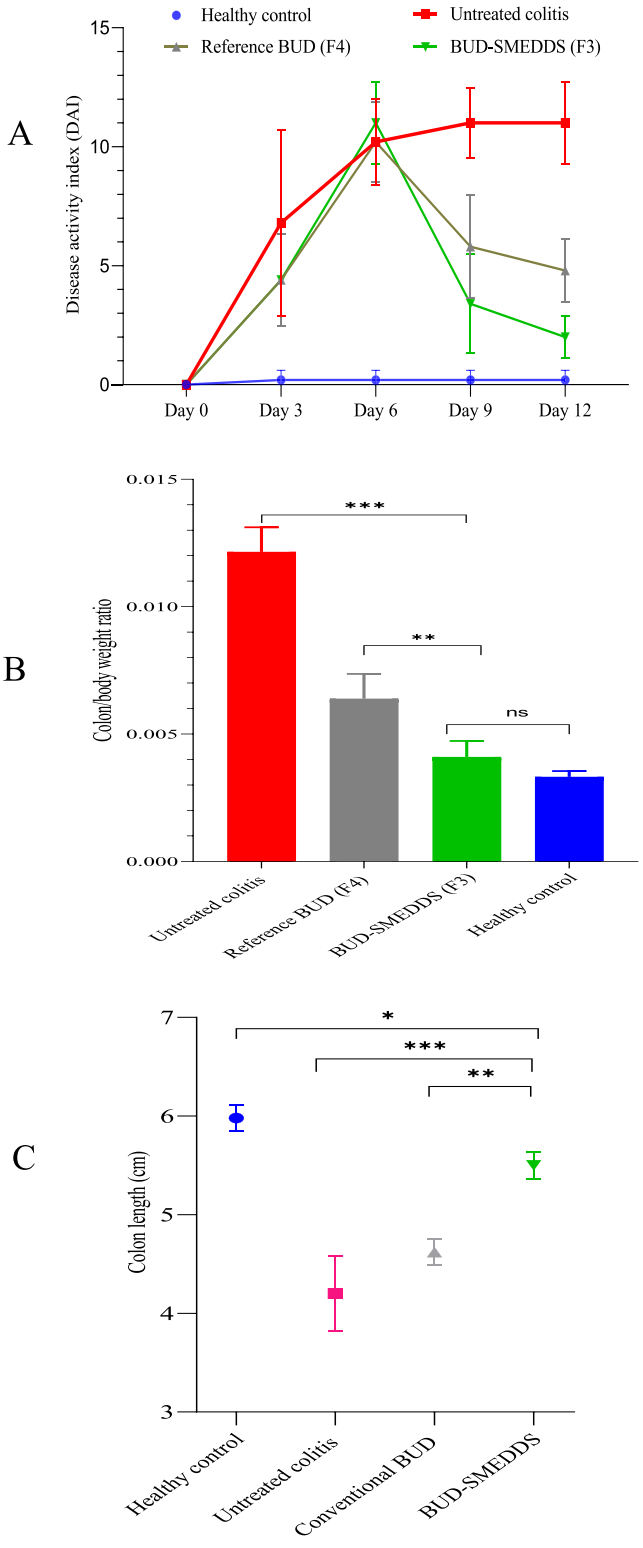

Figure 11 Disease activity index (**A**), colon/body weight ratio (**B**) and colon lengths (**C**) of tested animal groups.
Note: *p<0.05 **p<0.01, ***p<0.001.
Abbreviation: ns=non-significant

reference BUD and the BUD-SMEDDS formulations, respectively. A significant improvement was detected in BUD-SMEDDS compared to the reference BUD therapy ($p < 0.001$). Incorporation of BUD within a self-microemulsifying system (F3) positively assists the efficacy towards BUD in colitis. Histopathological assessment revealed a lower

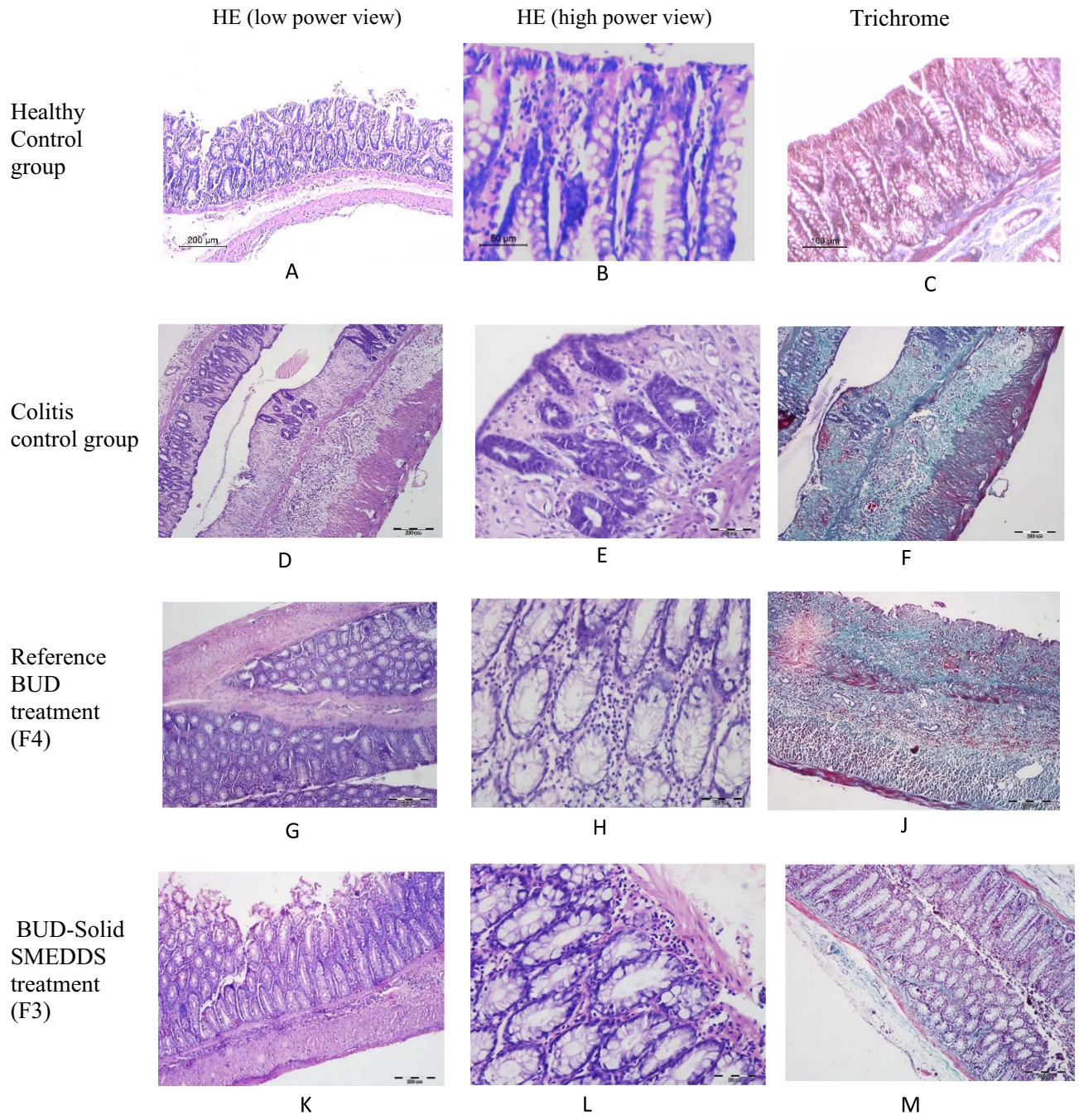

Figure 12 Photomicrographs of representative stained colonic tissues of tested groups. The first row; Photomicrographs of healthy colons stained by H&E at low power view (**A**), high power view (**B**), and trichrome stained (**C**). The second row; photomicrographs of colitis control colons stained by H&E at low-power view (**D**), high-power view (**E**), and trichrome stained (**F**). The third row; photomicrographs of H&E-stained colons treated by reference budesonide formulation at low-power view (**G**), and high-power view (**H**) and by trichrome stain (**J**). The fourth row; photomicrographs of H&E-stained colons treated by budesonide SMEDDS formulation at low power view (**K**), and high-power view (**L**) and by trichrome stain (**M**).

incidence of surface erosion and ulceration, reduced fibrosis of the lamina propria (predominantly responsible for chronic manifestations), and, most importantly, reversal of precancerous dysplastic changes. Furthermore, the mucoadhesive qualities of the Lutrols increased the possibility of BUD placement in the afflicted inflammatory areas, allowing for a greater intimate interaction between the medication and the injured mucosa. Lutrols can be considered intelligent polymers because they are thermosensitive; they undergo sol-gel transformation, especially Lutrol F127. The viscosity reached a maximum when the temperature was 30–60 ˚C. This allows for better mucoadhesion, especially in the layer in

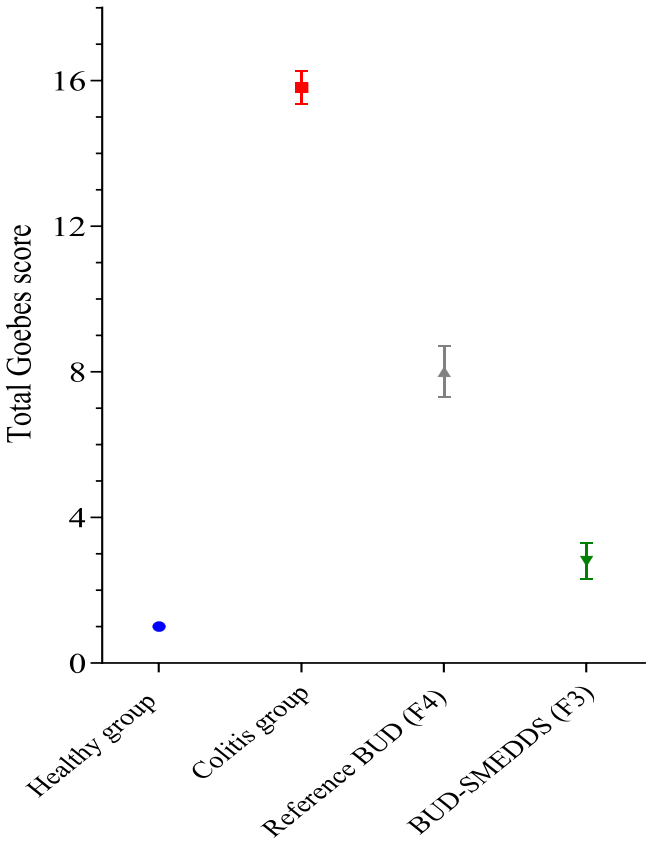

Figure 13 Total Geboes score of tested animal groups.
Notes: ns=non-significant, *p<0.05 **p<0.01, ***p<0.001.

contact with the colon.[79] The prolonged release of sufficient BUD concentrations from F3 enhanced the amelioration of colitis. Previous studies have demonstrated the cytoprotective and anti-inflammatory properties of poloxamers. Poloxamer 188 plays an important role in reducing environmental toxin damage and improving neuroinflammation.[80] Topical application of the Pluronic F-127 hydrogel to open excision wounds stimulates the production of VEGF and TGF-β1, resulting in improved wound healing.[81] Likewise, Pluronic F127 assisted BUD to distribute and penetrate tissues effectively in mice with inflammatory bowel diseases provoked by trinitrobenzenesulfonic acid, leading to a greater influence on local inflammation of the colorectal tissue.[82]

Stability

The overall stability test results indicated good physical stability of the tested formulation (F3). The formulation retained the original parameters of the freshly prepared formulation (Table 10). When dispersed, the stored F3 showed AGS, PDI and ZP values of 32 ± 4.1 nm, 0.34 ± 0.04, −20.4 ± 2.5 mV, respectively, signifying insignificant changes with the fresh

Table 10 Physicochemical Parameters for Fresh and Stored BUD-SMEDDS Formulation (F3)

Parameter	AGS (after redispersion, nm)	PDI (after redispersion)	ZP (mV)	Drug content (%)	% $Q_{120\ min}$
Before storage	29 ± 1.2	0.30 ± 0.02	− 22.4 ± 1.7	97.5 ± 6.3	36 ± 1.5
After 12 months storage	32 ± 4.1	0.34 ± 0.04	−20.4 ± 2.5	95.3 ± 7.5	34 ± 2.9

Abbreviations: Average globule size (AGS), Polydispersity index (PDI), Zeta potential (ZP), Percent drug released at 120 minutes (% $Q_{120\ min}$).

preparation ($p > 0.05$). In addition, BUD content after 12 months and % $Q_{120\ min}$ showed a slight change compared with the fresh sample.

Conclusion

Solid self-microemulsified budesonide delivery systems (BUD-SMEDDS) with droplet sizes less than 100 nm have been successfully developed. The Box–Behnken design was successfully utilized to optimize formulation of BUD-SMEDDS. Lutrol®-based suppositories were developed and characterized using the optimized values of ingredients. The potential of BUD-SMEDDS suppositories to combat distal forms of colitis was confirmed in an experimental colitis model. The integrated characteristics BUD SMEDDS help extend the formulations' residence time and maximize medication availability to the affected colitis areas. Based on these findings, BUD-SMEDDS can be viewed as a potential local therapy for distal ulcerative colitis. Further toxicological research is needed to assess the safety of the developed formulation.

Acknowledgment

The authors extend their appreciation to the Deputyship for Research & Innovation, Ministry of Education in Saudi Arabia, for funding this research through project number 445-9-270.

Funding

This research was funded by the Deputyship for Research & Innovation, Ministry of Education in Saudi Arabia, Saudi Arabia (No. 445-9-270).

Disclosure

The authors report no conflicts of interest in this work.

References

1. Rahimi R, Nikfarl S, Rezaie A, Abdollahi M. A meta-analysis of the benefit of probiotics in maintaining remission of human ulcerative colitis: evidence for prevention of disease relapse and maintenance of remission. *Arch Med Sci*. 2008;4(2):185–190.
2. Sandborn WJ, Travis S, Moro L, et al. Once-daily budesonide MMX(R) extended-release tablets induce remission in patients with mild to moderate ulcerative colitis: results from the CORE I study. *Gastroenterology*. 2012;143(5):1218–26e1–2. doi:10.1053/j.gastro.2012.08.003
3. Rogler G. Medical management of ulcerative colitis. *Dig Dis*. 2009;27(4):542–549. doi:10.1159/000233295
4. Danese S, Vuitton L, Peyrin-Biroulet L. Biologic agents for IBD: practical insights. *Nat Rev Gastroenterol Hepatol*. 2015;12(9):537–545. doi:10.1038/nrgastro.2015.135
5. Faubion WA, Loftus EV, Harmsen WS, Zinsmeister AR, Sandborn WJ. The natural history of corticosteroid therapy for inflammatory bowel disease: a population-based study. *Gastroenterology*. 2001;121(2):255–260. doi:10.1053/gast.2001.26279
6. Barrett K, Saxena S, Pollok R. Using corticosteroids appropriately in inflammatory bowel disease: a guide for primary care. *Br J Gen Pract*. 2018;68(675):497–498. doi:10.3399/bjgp18X699341
7. Deventer K, Mikulčíková P, Van Hoecke H, Van Eenoo P, Delbeke FT. Detection of budesonide in human urine after inhalation by liquid chromatography–mass spectrometry. *J Pharma Biome Ana*. 2006;42(4):474–479. doi:10.1016/j.jpba.2006.05.016
8. Ali HSM, York P, Blagden N, Soltanpour S, Acree WE Jr, Jouyban A. Solubility of Budesonide, Hydrocortisone, and Prednisolone in Ethanol + Water Mixtures at 298.2 K. *J Chem Eng Data*. 2010;55(1):578–582. doi:10.1021/je900376r
9. Bodas DS, Ige PP. Central composite rotatable design for optimization of budesonide-loaded cross-linked chitosan–dextran sulfate nanodispersion: characterization, in vitro diffusion and aerodynamic study. *Drug Dev. Ind. Pharm.* 2019;45(7):1193–1204. doi:10.1080/03639045.2019.1606823
10. Soltani F, Kamali H, Akhgari A, Garekani HA, Nokhodchi A, Sadeghi F. Different trends for preparation of budesonide pellets with enhanced dissolution rate. *Adv. Powder Technol.* 2022;33(8):103684. doi:10.1016/j.apt.2022.103684
11. Salunke A, Upmanyu N. Formulation, Development and Evaluation of Budesonide Oral Nano-sponges Using DOE Approach: in Vivo Evidences. *Adv Pharm Bull*. 2021;11(2):286–294. doi:10.34172/apb.2021.041
12. Hanauer SB, Robinson M, Pruitt R, et al. Budesonide enema for the treatment of active, distal ulcerative colitis and proctitis: a dose-ranging study. *Gastroenterology*. 1998;115(3):525–532. doi:10.1016/S0016-5085(98)70131-3
13. Gross V, Bar-Meir S, Lavy A, et al. The International Budesonide Foam Study G. Budesonide foam versus budesonide enema in active ulcerative proctitis and proctosigmoiditis. *Aliment. Pharmacol. Ther.* 2006;23(2):303–312. doi:10.1111/j.1365-2036.2006.02743.x
14. Sandborn WJ, Bosworth B, Zakko S, et al. Budesonide Foam Induces Remission in Patients With Mild to Moderate Ulcerative Proctitis and Ulcerative Proctosigmoiditis. *Gastroenterology*. 2015;148(4):740–750.e2. doi:10.1053/j.gastro.2015.01.037
15. Kim YH, Kim SB, Choi SH, et al. Development and Evaluation of Self-Microemulsifying Drug Delivery System for Improving Oral Absorption of Poorly Water-Soluble Olaparib. *Pharmaceutics*. 2023;15(6). doi:10.3390/pharmaceutics15061669
16. Venkata Ramana Rao S, Shao J. Self-nanoemulsifying drug delivery systems (SNEDDS) for oral delivery of protein drugs: i. Formulation development. *Int J Pharm*. 2008;362(1–2):2–9. doi:10.1016/j.ijpharm.2008.05.018

17. Soliman KA, Ibrahim HK, Ghorab MM. Formulation of avanafil in a solid self-nanoemulsifying drug delivery system for enhanced oral delivery. *Eur. J. Pharm. Sci.* 2016;93:447–455. doi:10.1016/j.ejps.2016.08.050
18. Ali HSM, Ahmed SA, Alqurshi AA, Alalawi AM, Shehata AM, Alahmadi YM. Tadalafil-Loaded Self-Nanoemulsifying Chewable Tablets for Improved Bioavailability: design, In Vitro, and In Vivo Testing. *Pharmaceutics*. 2022;14(9):1927.
19. Parmar K, Patel J, Sheth N. Self nano-emulsifying drug delivery system for Embelin: design, characterization and in-vitro studies. *Asian J Pharm Sci*. 2015;10(5):396–404. doi:10.1016/j.ajps.2015.04.006
20. Lee DW, Marasini N, Poudel BK, et al. Application of Box-Behnken design in the preparation and optimization of fenofibrate-loaded self-microemulsifying drug delivery system (SMEDDS). *J Microencapsul*. 2014;31(1):31–40. doi:10.3109/02652048.2013.805837
21. Hou S, Hindle M, Byron PR. A stability-indicating HPLC assay method for budesonide. *J Pharma Biome Ana*. 2001;24(3):371–380. doi:10.1016/S0731-7085(00)00424-6
22. Ali HSM, Ahmed SA, Alqurshi AA, Alalawi AM, Shehata AM, Alahmadi YM. Boosting Tadalafil Bioavailability via Sono-Assisted Nano-Emulsion-Based Oral Jellies: box–Behnken Optimization and Assessment. *Pharmaceutics*. 2022;14(12):2592.
23. Kim DS, Cho JH, Park JH, et al. Self-microemulsifying drug delivery system (SMEDDS) for improved oral delivery and photostability of methotrexate. *Int J Nanomed*. 2019;14:4949–4960. doi:10.2147/ijn.S211014
24. Patel J, Dhingani A, Garala K, Raval M, Sheth N. Quality by design approach for oral bioavailability enhancement of irbesartan by self-nanoemulsifying tablets. *Drug Deliv*. 2014;21(6):412–435. doi:10.3109/10717544.2013.853709
25. Kalhapure RS, Akamanchi KG. Oleic acid based heterolipid synthesis, characterization and application in self-microemulsifying drug delivery system. *Int J Pharm*. 2012;425(1):9–18. doi:10.1016/j.ijpharm.2012.01.004
26. Wang Q, Guo M, Adu-Frimpong M, et al. Self-Micro-Emulsifying Controlled Release of Eugenol Pellets: preparation, In vitro/In vivo Investigation in Beagle Dogs. *AAPS Pharm Sci Tech*. 20(7):284. doi:10.1208/s12249-019-1499-4
27. Kumar M, Bishnoi RS, Shukla AK, Jain CP. Development and optimization of drug-loaded nanoemulsion system by phase inversion temperature (PIT) method using Box–Behnken design. *Drug Dev. Ind. Pharm*. 2021;47(6):977–989. doi:10.1080/03639045.2021.1957920
28. Aqil M, Kamran M, Ahad A, Imam SS. Development of clove oil based nanoemulsion of olmesartan for transdermal delivery: box–Behnken design optimization and pharmacokinetic evaluation. *J Mol Liq*. 2016;214:238–248. doi:10.1016/j.molliq.2015.12.077
29. Usta DY, Timur B, Teksin ZS. Formulation development, optimization by Box-Behnken design, characterization, in vitro, ex-vivo, and in vivo evaluation of bosentan-loaded self-nanoemulsifying drug delivery system: a novel alternative dosage form for pulmonary arterial hypertension treatment. *Eur. J. Pharm. Sci.* 2022;174:106159. doi:10.1016/j.ejps.2022.106159
30. Yadav P, Rastogi V, Verma A. Application of Box–Behnken design and desirability function in the development and optimization of self-nanoemulsifying drug delivery system for enhanced dissolution of ezetimibe. *Future J Pharm Sci*. 2020;6(1):7. doi:10.1186/s43094-020-00023-3
31. Goh PS, Ng MH, Choo YM, Amru NB, Chuah CH. Production of Nanoemulsions from Palm-Based Tocotrienol Rich Fraction by Microfluidization. *Molecules*. 2015;20(11):19936–19946.
32. Ali HH, Hussein AA. Oral nanoemulsions of candesartan cilexetil: formulation, characterization and in vitro drug release studies. *AAPS Open*. 2017;3(1):4. doi:10.1186/s41120-017-0016-7
33. Azeem A, Rizwan M, Ahmad FJ, et al. Nanoemulsion Components Screening and Selection: a Technical Note. *AAPS Pharm Sci Tech*. 2009;10(1):69–76. doi:10.1208/s12249-008-9178-x
34. Ali HSM, Hanafy AF, El Achy SN. Tailoring the mucoadhesive and sustained release characteristics of mesalamine loaded formulations for local treatment of distal forms of ulcerative colitis. *Eur. J. Pharm. Sci.* 2016;93:233–243. doi:10.1016/j.ejps.2016.08.008
35. Zidan AS, Emam SE, Shehata TM, Ghazy FE. Pediatric suppositories of sulpiride solid dispersion for treatment of Tourette syndrome: in vitro and in vivo investigations. *AAPS Pharm Sci Tech*. 2015;16(3):645–655. doi:10.1208/s12249-014-0250-4
36. Teaima MH, El Mohamady AM, El-Nabarawi MA, Mohamed AI. Formulation and evaluation of niosomal vesicles containing ondansetron HCL for trans-mucosal nasal drug delivery. *Drug Dev. Ind. Pharm.* 2020;46(5):751–761. doi:10.1080/03639045.2020.1753061
37. Koirala S, Nepal P, Ghimire G, et al. Formulation and evaluation of mucoadhesive buccal tablets of aceclofenac. *Heliyon*. 2021;7(3):e06439. doi:10.1016/j.heliyon.2021.e06439
38. Patil J. Formulation, characterization and in vivo evaluation of novel edible dosage form containing nebivolol HCl. *Brazilian J Pharm Sciences*. 2016.
39. Arora G, Malik K, Singh I. Formulation and evaluation of mucoadhesive matrix tablets of taro gum: optimization using response surface methodology. *Polim Med*. 2011;41(2):23–34.
40. Colpo JC, Pigatto C, Brizuela N, Aragón J, Dos Santos LAL. Antibiotic and anesthetic drug release from double-setting α-TCP cements. *J Mater Sci*. 2018;53(10):7112–7124. doi:10.1007/s10853-018-2071-4
41. Takhshid MA, Mehrabani D, Ai J, Zarepoor M. The healing effect of licorice extract in acetic acid-induced ulcerative colitis in rat model. *Comp Clin Pathol*. 2012;21(6):1139–1144. doi:10.1007/s00580-011-1249-9
42. Bitiren M, Karakilcik AZ, Zerin M, et al. Protective Effects of Selenium and Vitamin E Combination on Experimental Colitis in Blood Plasma and Colon of Rats. *Biol. Trace Elem. Res.* 2010;136(1):87–95. doi:10.1007/s12011-009-8518-3
43. Mondal S, Das M, Ghosh R, et al. Chitosan functionalized Mn3O4 nanoparticles counteracts ulcerative colitis in mice through modulation of cellular redox state. *Commun. Biol.* 2023;6(1):647. doi:10.1038/s42003-023-05023-6
44. Jeengar MK, Thummuri D, Magnusson M, Naidu VGM, Uppugunduri S. Uridine Ameliorates Dextran Sulfate Sodium (DSS)-Induced Colitis in Mice. *Sci Rep*. 2017;7(1):3924. doi:10.1038/s41598-017-04041-9
45. Jauregui-Amezaga A, Geerits A, Das Y, et al. A Simplified Geboes Score for Ulcerative Colitis. *J Crohns Colitis*. 11(3):305–313. doi:10.1093/ecco-jcc/jjw154
46. Yousry C, Zikry PM, Basalious EB, El-Gazayerly ON. Self-nanoemulsifying System Optimization for Higher Terconazole Solubilization and Non-Irritant Ocular Administration. *Adv Pharm Bull*. 2020;10(3):389–398. doi:10.34172/apb.2020.047
47. Balakrishnan P, Lee B-J, Oh DH, et al. Enhanced oral bioavailability of dexibuprofen by a novel solid Self-emulsifying drug delivery system (SEDDS). *Eur. J. Pharm. Biopharm.* 2009;72(3):539–545. doi:10.1016/j.ejpb.2009.03.001
48. Abd-Elhakeem E, Teaima MHM, Abdelbary GA, El Mahrouk GM. Bioavailability enhanced clopidogrel -loaded solid SNEDDS: development and in-vitro/in-vivo characterization. *J Drug Delivery Sci Technol*. 2019;49:603–614. doi:10.1016/j.jddst.2018.12.027

49. Lawrence MJ, Rees GD. Microemulsion-based media as novel drug delivery systems. *Adv Drug Deliv Rev*. 45(1):89–121. doi:10.1016/s0169-409x(00)00103-4
50. Zhang P, Liu Y, Feng N, Xu J. Preparation and evaluation of self-microemulsifying drug delivery system of oridonin. *Int J Pharm*. 355(1–2):269–276. doi:10.1016/j.ijpharm.2007.12.026
51. Sharma S, Narang JK, Ali J, Baboota S. Synergistic antioxidant action of vitamin E and rutin SNEDDS in ameliorating oxidative stress in a Parkinson's disease model. *Nanotechnology*. 27(37):375101. doi:10.1088/0957-4484/27/37/375101
52. Cho HJ, Lee DW, Marasini N, et al. Optimization of self-microemulsifying drug delivery system for telmisartan using Box-Behnken design and desirability function. *J Pharm Pharmacol*. 2013;65(10):1440–1450. doi:10.1111/jphp.12115
53. Li H, Pan T, Cui Y, et al. Improved oral bioavailability of poorly water-soluble glimepiride by utilizing microemulsion technique. *Int J Nanomed*. 2016;11:3777–3788. doi:10.2147/ijn.S105419
54. Shanmugam S, Baskaran R, Balakrishnan P, Thapa P, Yong CS, Yoo BK. Solid self-nanoemulsifying drug delivery system (S-SNEDDS) containing phosphatidylcholine for enhanced bioavailability of highly lipophilic bioactive carotenoid lutein. *Eur. J. Pharm. Biopharm.* 2011;79(2):250–257. doi:10.1016/j.ejpb.2011.04.012
55. Leichner C, Baus RA, Jelkmann M, et al. In vitro evaluation of a self-emulsifying drug delivery system (SEDDS) for nasal administration of dimenhydrinate. *Drug Deliv Transl Res*. 2019;9(5):945–955. doi:10.1007/s13346-019-00634-1
56. Mehrnia M-A, Jafari S-M, Makhmal-Zadeh BS, Maghsoudlou Y. Crocin loaded nano-emulsions: factors affecting emulsion properties in spontaneous emulsification. *Int J Biol Macromol*. 2016;84:261–267. doi:10.1016/j.ijbiomac.2015.12.029
57. Ali HSM, Ahmed SA, Alqurshi AA, Alalawi AM, Shehata AM, Alahmadi YM. Boosting Tadalafil Bioavailability via Sono-Assisted Nano-Emulsion-Based Oral Jellies: box-Behnken Optimization and Assessment. *Pharmaceutics*. 2022;14(12). doi:10.3390/pharmaceutics14122592
58. Zafar A, Yasir M, Alruwaili NK, et al. Formulation of Self-Nanoemulsifying Drug Delivery System of Cephalexin: physiochemical Characterization and Antibacterial Evaluation. *Polymers*. 2022;14(5):1055.
59. Sarheed O, Dibi M, KVRNS R. Studies on the Effect of Oil and Surfactant on the Formation of Alginate-Based O/W Lidocaine Nanocarriers Using Nanoemulsion Template. *Pharmaceutics*. 2020;12(12):1223. doi:10.3390/pharmaceutics12121223
60. Yuan Y, Cui Y, Zhang L, et al. Thermosensitive and mucoadhesive in situ gel based on poloxamer as new carrier for rectal administration of nimesulide. *Int J Pharm*. 2012;430(1):114–119. doi:10.1016/j.ijpharm.2012.03.054
61. Barakat NS. In vitro and in vivo characteristics of a thermogelling rectal delivery system of etodolac. *AAPS Pharm Sci Tech*. 2009;10(3):724–731. doi:10.1208/s12249-009-9261-y
62. Karami Z, Zanjani MS, Andalib S, Babaie H, Aminoroaia P. Influence of Poloxamer 188 on Anti-Inflammatory and Analgesic Effects of Diclofenac-Loaded Nanoemulsion: formulation, Optimization and in Vitro/in Vivo Evaluation. *J Pharm Sci*. 2023;112(12):3197–3208. doi:10.1016/j.xphs.2023.09.022
63. Cheng Y-H, Fung M-P, Chen Y-Q, Chiu Y-C. Development of mucoadhesive methacrylic anhydride-modified hydroxypropyl methylcellulose hydrogels for topical ocular drug delivery. *J Drug Delivery Sci Technol*. 2024;93:105450. doi:10.1016/j.jddst.2024.105450
64. Diaz-Salmeron R, Toussaint B, Huang N, et al. Mucoadhesive Poloxamer-Based Hydrogels for the Release of HP-β-CD-Complexed Dexamethasone in the Treatment of Buccal Diseases. *Pharmaceutics*. 2021;13(1). doi:10.3390/pharmaceutics13010117
65. Giuliano E, Paolino D, Fresta M, Cosco D. Mucosal Applications of Poloxamer 407-Based Hydrogels: an Overview. *Pharmaceutics*. 2018;10(3):159.
66. Baloglu E, Karavana SY, Senyigit ZA, Guneri T. Rheological and mechanical properties of poloxamer mixtures as a mucoadhesive gel base. *Pharma DevelopTechn*. 2011;16(6):627–636. doi:10.3109/10837450.2010.508074
67. Tuğcu Demiröz FN, Ongun M, Tunçel E, Kodan E, Tırnaksız FF. Development and characterization of mucoadhesive -thermosensitive buccal gel containing metronidazole for the treatment of oral mucositis. Oral mukozİt tedavİsİ İÇİn metronİdazol İÇeren mukoadezİf-termosensİtİf buccal jelİn gelİŞtİrİlmesİ ve karakterİzasyonu. *J Fac Pharm Ankara Unive*. 2020;44(3):517–539. doi:10.33483/jfpau.742957
68. Mansour M, Mansour S, Mortada ND, Abd Elhady SS. Ocular poloxamer-based ciprofloxacin hydrochloride in situ forming gels. *Drug Dev Ind Pharm*. 2008;34(7):744–752. doi:10.1080/03639040801926030
69. Leng D, Kissi EO, Löbmann K, et al. Design of Inhalable Solid Dosage Forms of Budesonide and Theophylline for Pulmonary Combination Therapy. *AAPS Pharm Sci Tech*. 20(3):137. doi:10.1208/s12249-019-1344-9
70. Mezzena M, Scalia S, Young PM, Traini D. Solid lipid budesonide microparticles for controlled release inhalation therapy. *Aaps j*. 2009;11(4):771–778. doi:10.1208/s12248-009-9148-6
71. Szafraniec J, Antosik A, Knapik-Kowalczuk J, et al. The Self-Assembly Phenomenon of Poloxamers and Its Effect on the Dissolution of a Poorly Soluble Drug from Solid Dispersions Obtained by Solvent Methods. *Pharmaceutics*. 2019;11(3). doi:10.3390/pharmaceutics11030130
72. Shah AV, Serajuddin AT. Development of solid self-emulsifying drug delivery system (SEDDS) I: use of poloxamer 188 as both solidifying and emulsifying agent for lipids. *Pharm Res*. 2012;29(10):2817–2832. doi:10.1007/s11095-012-0704-x
73. Zarrintaj P, Ramsey JD, Samadi A, et al. Poloxamer: a versatile tri-block copolymer for biomedical applications. *Acta Biomater.* 2020;110:37–67. doi:10.1016/j.actbio.2020.04.028
74. Abdeltawab H, Svirskis D, Sharma M. Formulation strategies to modulate drug release from poloxamer based in situ gelling systems. *Expert Opin Drug Delivery*. 2020;17(4):495–509. doi:10.1080/17425247.2020.1731469
75. Mahapatra AK, Sameeraja NH, Murthy PN. Development of modified-release tablets of zolpidem tartrate by biphasic quick/slow delivery system. *AAPS Pharm Sci Tech*. 2015;16(3):579–588. doi:10.1208/s12249-014-0236-2
76. Bermúdez JM, Jimenez-Kairuz AF, Olivera ME, Allemandi DA, Manzo RH. A ciprofloxacin extended release tablet based on swellable drug polyelectrolyte matrices. *AAPS Pharm Sci Tech*. 2008;9(3):924–930. doi:10.1208/s12249-008-9098-9
77. Chassaing B, Aitken JD, Malleshappa M, Vijay-Kumar M. Dextran sulfate sodium (DSS)-induced colitis in mice. *Curr Protoc Immunol*. 2014.104;15.25.1–15.25.14. doi:10.1002/0471142735.im1525s104
78. Zidar N, Langner C, Jerala M, Boštjančič E, Drobne D, Tomažič A. Pathology of Fibrosis in Crohn's Disease—Contribution to Understanding Its Pathogenesis. Original Research. *Front Med*. 2020;7. doi:10.3389/fmed.2020.00167
79. Al Khateb K, Ozhmukhametova EK, Mussin MN, et al. In situ gelling systems based on Pluronic F127/Pluronic F68 formulations for ocular drug delivery. *Int J Pharm*. 2016;502(1):70–79. doi:10.1016/j.ijpharm.2016.02.027

80. Ding W, Lin H, Hong X, Ji D, Wu F. Poloxamer 188-mediated anti-inflammatory effect rescues cognitive deficits in paraquat and maneb-induced mouse model of Parkinson's disease. *Toxicology*. 2020. 436;152437. doi:10.1016/j.tox.2020.152437
81. Kant V, Gopal A, Kumar D, et al. Topical pluronic F-127 gel application enhances cutaneous wound healing in rats. *Acta Histochem*. 2014;116 (1):5–13. doi:10.1016/j.acthis.2013.04.010
82. Date AA, Halpert G, Babu T, et al. Mucus-penetrating budesonide nanosuspension enema for local treatment of inflammatory bowel disease. *Biomaterials*. 2018;185:97–105. doi:10.1016/j.biomaterials.2018.09.005